Electronic Supplementary Material (ESI) for Dalton Transactions.

Electronic Supplementary Information ESI

Non-symmetric sulfur-based O,C,O-chelating pincer ligand leading to chiral germylene and stannylene

Noemi Deak,[a,b] Olivier Thillaye du Boullay,[b] Ionut-Tudor Moraru,[a] Sonia Mallet-Ladeira,[c] David Madec,*[b] Gabriela Nemes*[a]

[a] Universitatea Babeş-Bolyai, Facultatea de Chimie şi Inginerie Chimică, str. Arany Janos, nr; 11, RO-400028, Cluj-Napoca, Romania.
[b] Université de Toulouse, UPS, LHFA, 118 Route de Narbonne, F-31062 Toulouse, France, CNRS, LHFA, UMR 5069, F-31062 Toulouse Cedex 9, France.
[c] Institut de Chimie de Toulouse, FR2599, Université Paul Sabatier, UPS, 118 Route de Narbonne, F-31062 Toulouse Cedex 9, France.

***corresponding authors:** gabriela.nemes@ubbcluj.ro, madec@chimie.ups-tlse.fr

Table of Contents

Additional details concerning compounds 1-3

The formation of the bromo-thioether **1** was evidenced by ^{1}H NMR spectroscopy, presenting three characteristic triplet signals for H1, H3 and H5 hydrogen atoms of the central aromatic ring at 7.10 (t, $^4J_{HH}$ = 1.69 Hz), 7.23 (t, $^4J_{HH}$ = 1.63 Hz) and 7.31-7.34 (m) ppm. The ^{1}H NMR analysis of compound **2**, obtained by oxidation of **1** shows the deshielding of the characteristic triplet signals for the aromatic hydrogen atoms, compared to compound **1**, the expected effect of the sulfoxide group. The signals of the H1, H3 and H5 hydrogen atoms shift from 7.10 (t, $^4J_{HH}$ = 1.69 Hz), 7.23 (t, $^4J_{HH}$ = 1.63 Hz), 7.31-7.34 (m) ppm in compound **1** to 7.48 (t, $^4J_{HH}$ = 1.65 Hz), 7.51-7.54 (m), 7.62 (t, $^4J_{HH}$ = 1.62 Hz) ppm in compound **2**. Single crystals suitable for X-ray analysis were obtained in CH_2Cl_2 solution of the bulk compound.

In compound **3**, because of the existence of two different functional groups (the sulfonyl and the sulfinyl), the symmetry seen in the bis-sulfone is no longer present. Thus, the signals of the hydrogen and carbon atoms in the ^{1}H and ^{13}C spectra (ex. the methyl groups or the H atoms on the tolyl groups) appear at different chemical shifts. Spectroscopic studies presented in literature, realized on different sulphide, sulfonyl or sulfinyl containing compounds, investigating the shielding and deshielding effect of these functional groups, show that the sulfone group has a greater deshielding effect on the adjacent aromatic or aliphatic moieties than the sulfoxide ones.[15-16] The downfield shift of the signals in ^{1}H NMR is an expected phenomenon because of the polarity of the sulfone and the sulfoxide group.

Upon a detailed study of the ^{1}H NMR data for the H1, H3 and H5 protons of the central aromatic ring a triplet signal was observed at 7.96 ppm (t, $^4J_{HH}$ = 1.72 Hz) and a doublet signal at 7.86 ppm (in $CDCl_3$, $^4J_{HH}$ = 1.73 Hz) at first assigned to the *meta* protons H3 and H5. This doublet signal for H3 and H5 seemed to be unusual, because they are not identical due to the existence of the two different sulfonyl and sulfinyl functional groups. Indeed, if a concentrated NMR sample was used, a triplet signal could be observed at 7.95 ppm (t, $^4J_{HH}$ = 1.70 Hz), at first assigned for H1, and two overlapped triplets at 7.86 and 7.87 ppm (t, $^4J_{HH}$ = 1.60 Hz, 1.65 Hz) instead of the previously seen doublet signal.

For further information, variable temperature ^{1}H NMR analysis was realized in $CDCl_3$. In the ^{1}H NMR spectra of the sulfone-sulfoxide **3** at -75 °C two triplet signals can be seen at 7.83 ($^4J_{HH}$ = 1.56 Hz) and 7.86 ($^4J_{HH}$ = 1.64) instead of a doublet signal, as expected for the compound. All these suggest a dynamic behavior of the sulfone-sulfoxide **3** due to the existence of both the sulfonyl and sulfinyl groups in the molecule. This could result in easier adaptability of the ligand which can play a role in the stabilization of the target metallylenes.

In order to assign these three triplet signals for the H1, H3 and H5 protons of sulfone-sulfoxide **3**, bidimensional NMR experiments (COSY, HSQC, HMBC) were employed, fragments of the HMBC and HSQC spectra are shown in Figure S9 in SI. In the HSQC spectrum a correlation can be seen between the signals at 121 ppm in ^{13}C NMR, assigned for the C1 carbon atom, and one of the signals from the doublet of triplets at 7.9 ppm. Furthermore, in the HMBC spectrum there is a correlation between the signal at 35 ppm in ^{13}C NMR, assigned for the quaternary carbon atom of the *tert*-butyl group ($C(CH_3)_3$) and both signals at 8.0 and 7.9 ppm. All these suggest that the triplet signal at 7.95 ppm is for one of the *meta* protons of the central aromatic ring (H3, H5) and the signal for the H1 proton is found at 7.87 ppm (t, $^4J_{HH}$ = 1.60 Hz).

In THF-D_8 the ^{1}H NMR spectrum of sulfone-sulfoxide **3** exhibits three triplet signals for the H1, H3 and H5 aromatic protons at 7.94 (t, 1H, J = 1.68 Hz), 7.98 (t, 1H, J = 1.74 Hz), 8.03 (t, 1H, J = 1.59 Hz). In the ^{1}H NMR spectra all the characteristic signals of the tolyl and of the central aromatic cyclic moieties can be identified.

NMR and mass analysis spectra

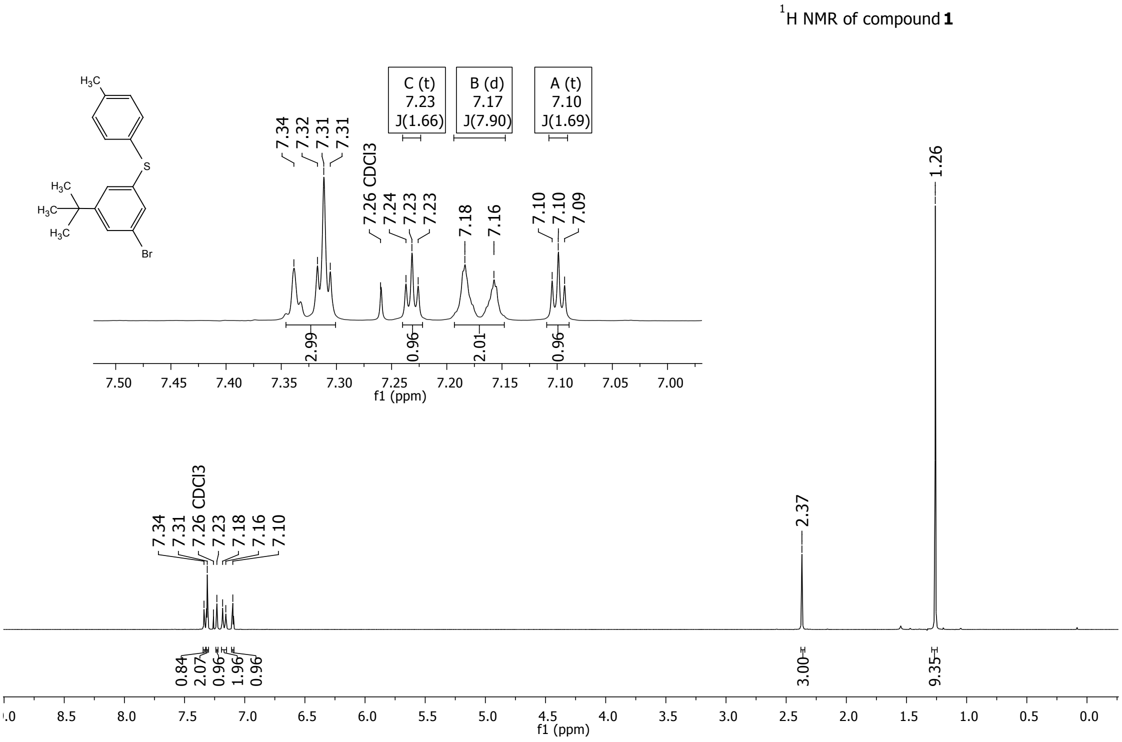

Figure S1. ^{1}H NMR spectrum of compound **1**

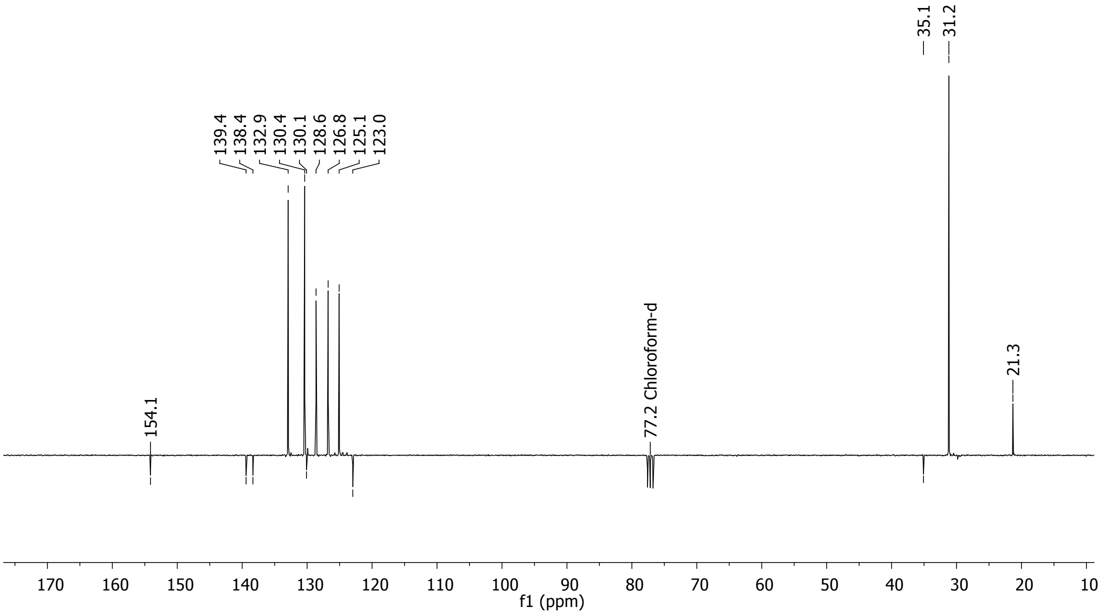

Figure S2. ^{13}C NMR spectrum of compound **1**

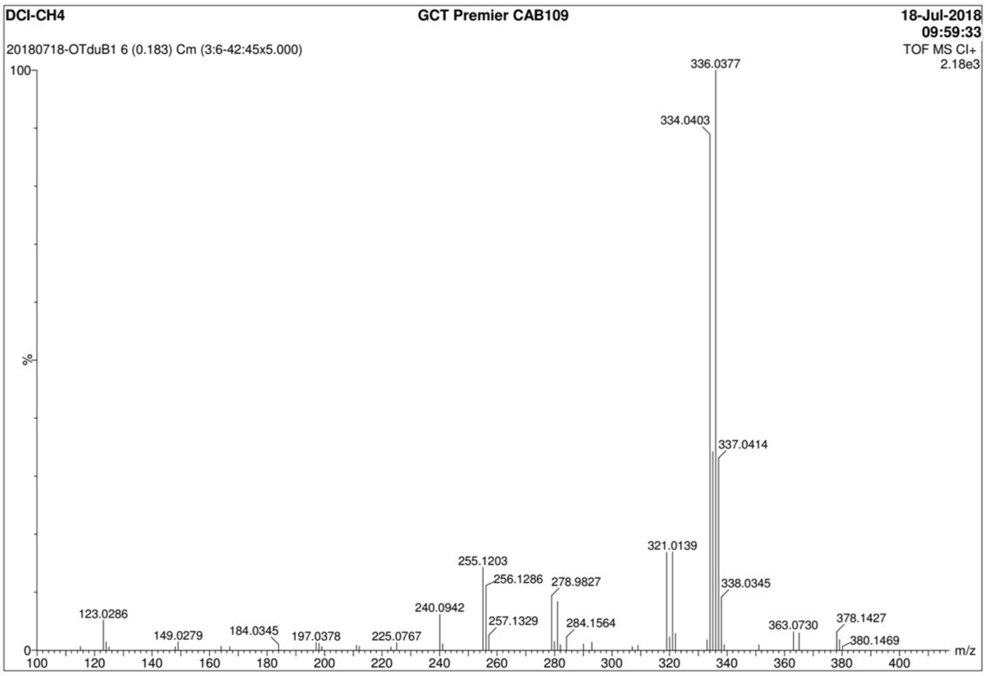

Figure S3. Mass spectrum of compound **1**

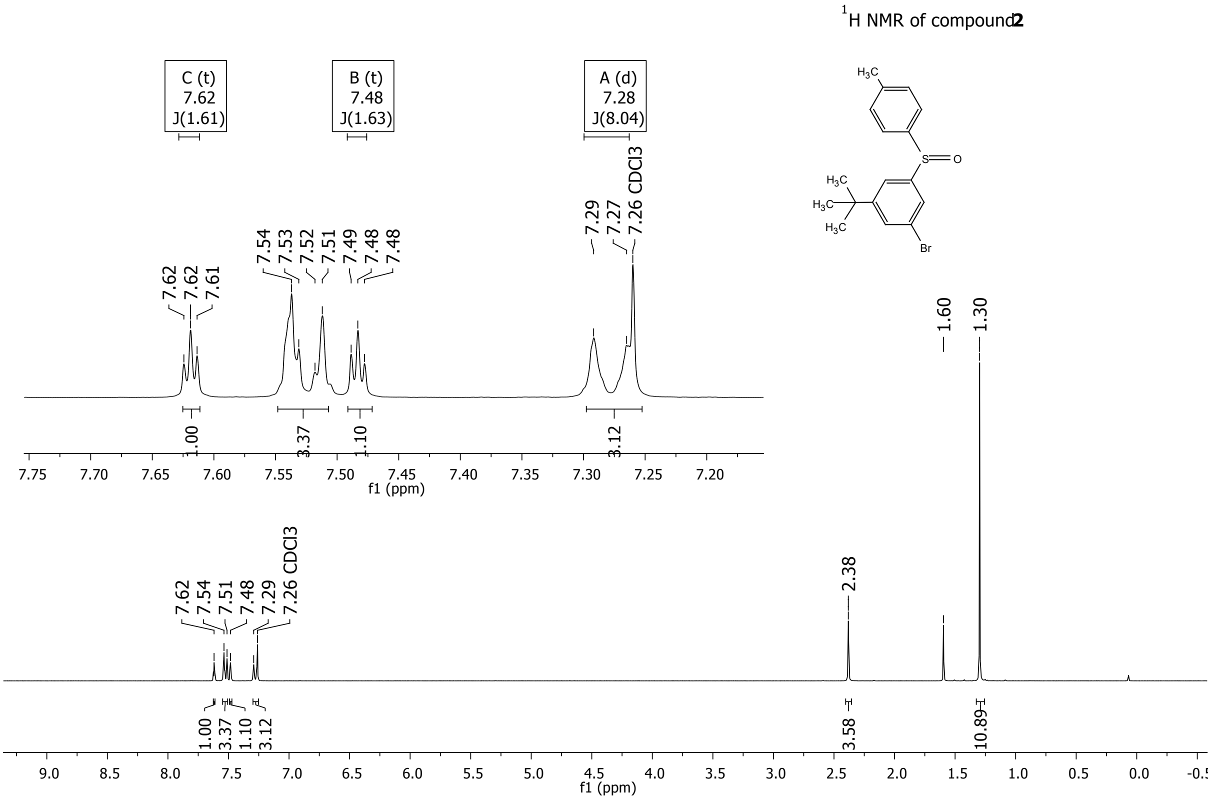

Figure S4. ^{1}H NMR spectrum of compound **2**

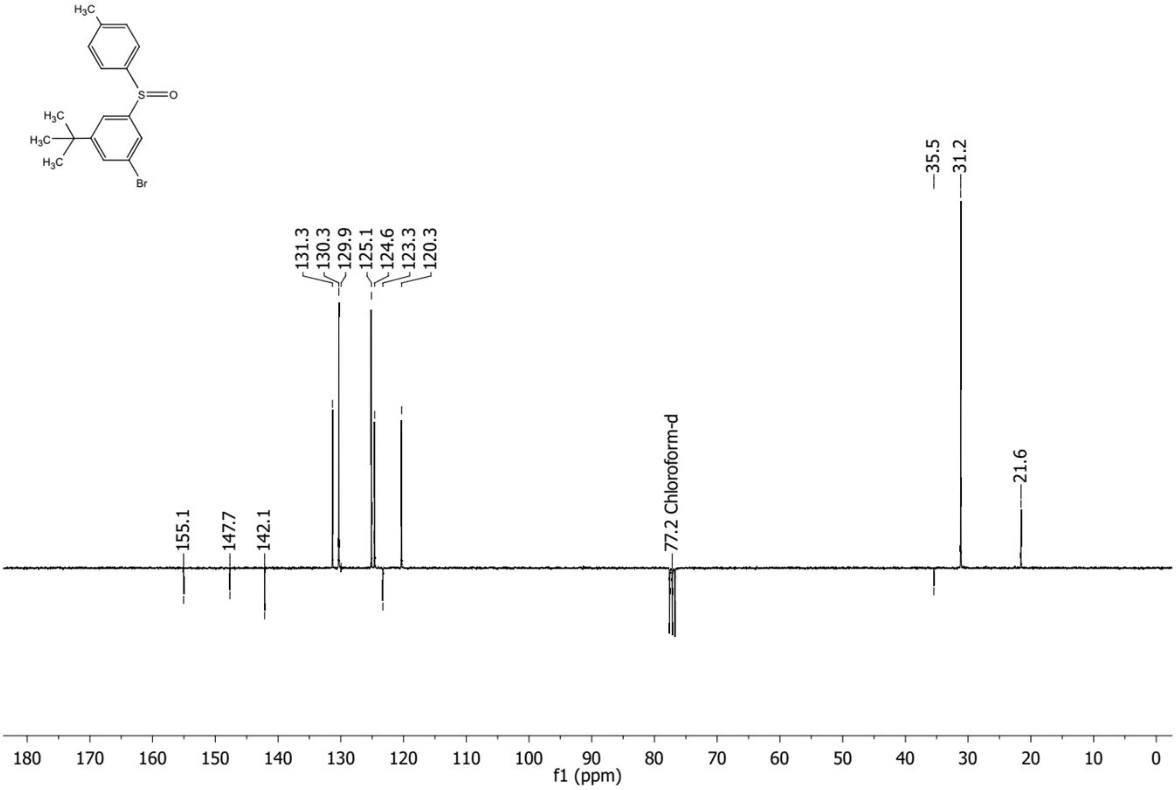

Figure S5. ^{13}C NMR spectrum of compound **2**

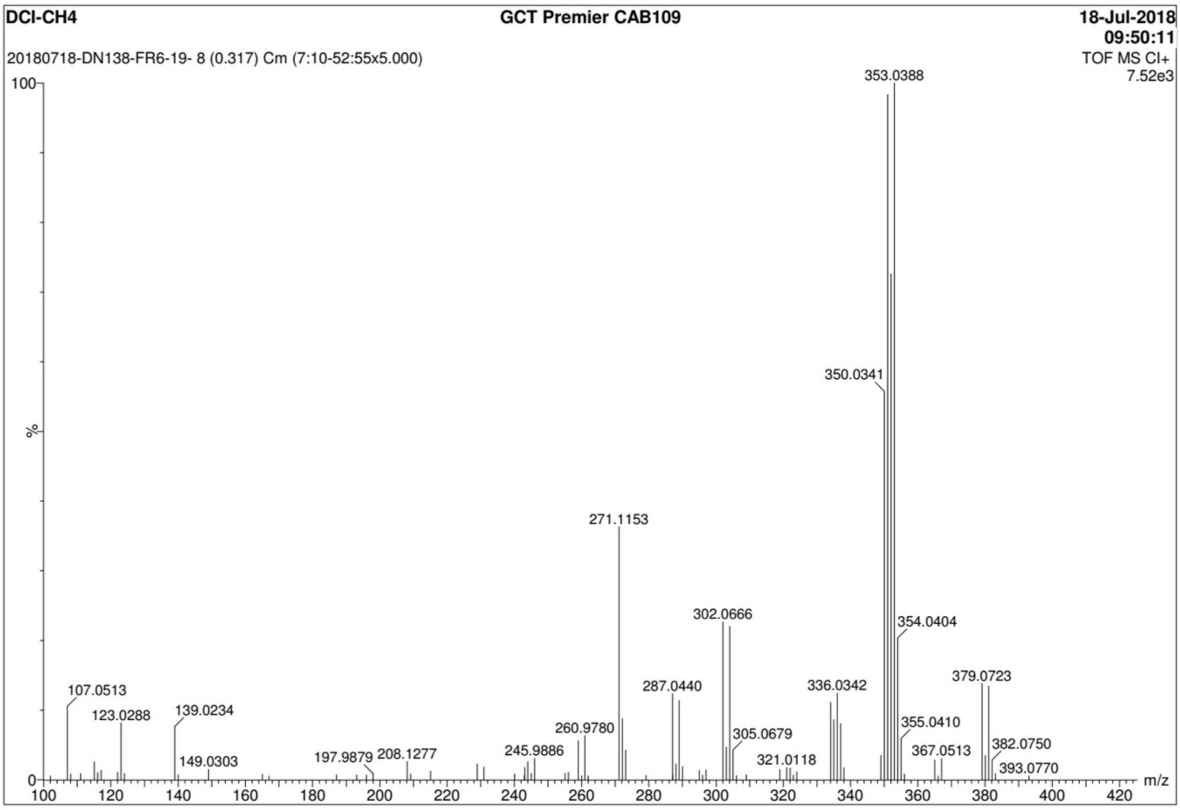

Figure S6. Mass spectrum of compound **2**

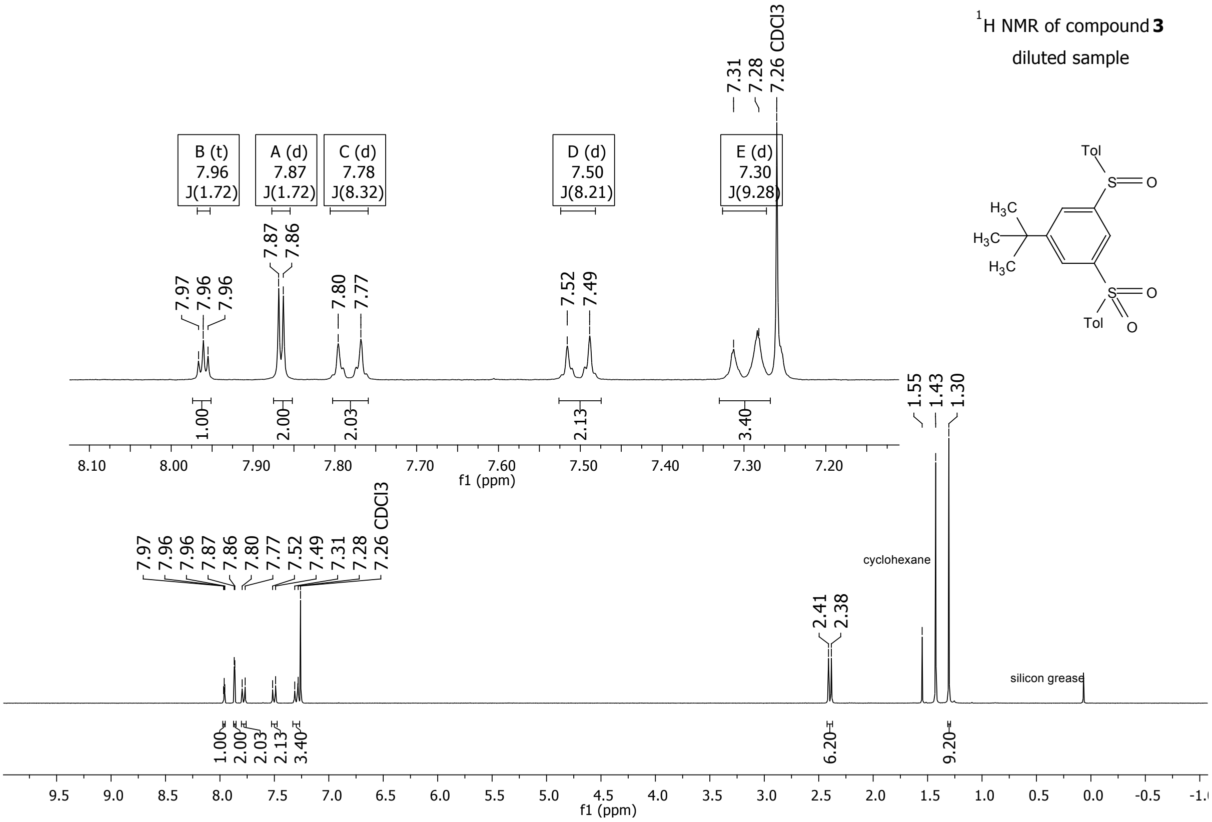

Figure S7. ^{1}H NMR spectrum of compound **3** in $CDCl_3$ on a diluted sample

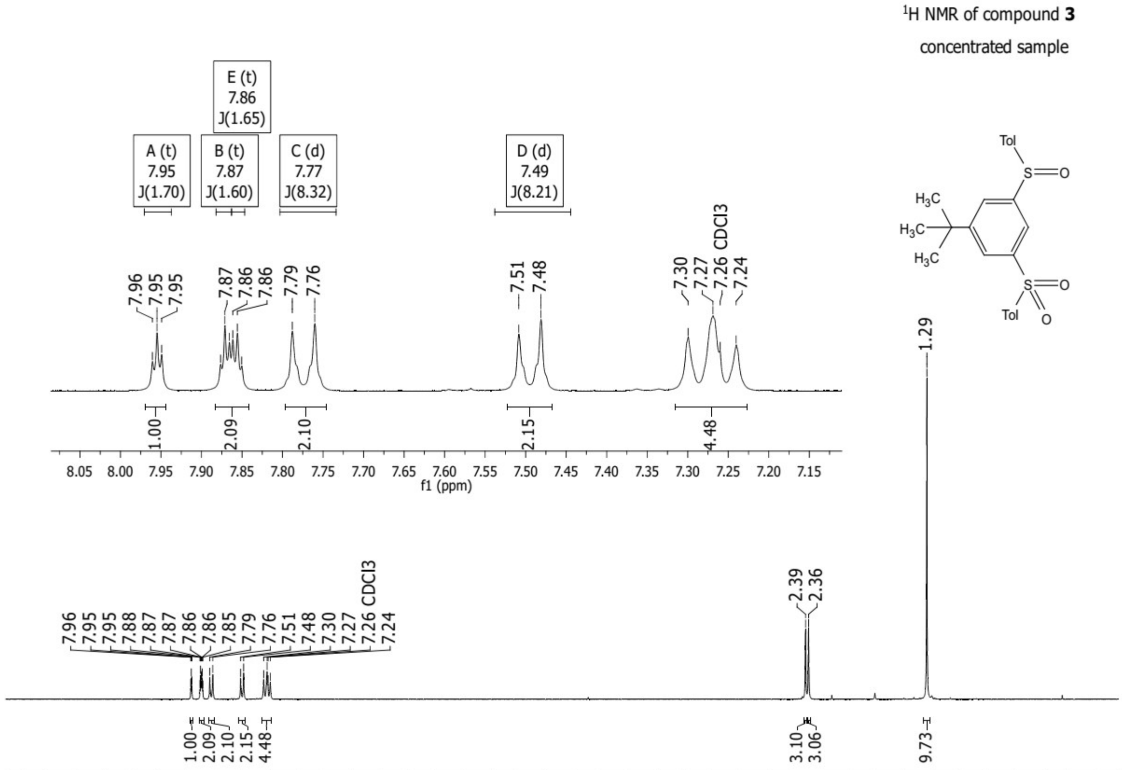

Figure S8. ^{1}H NMR spectrum of compound **3** in $CDCl_3$ on a concentrated sample

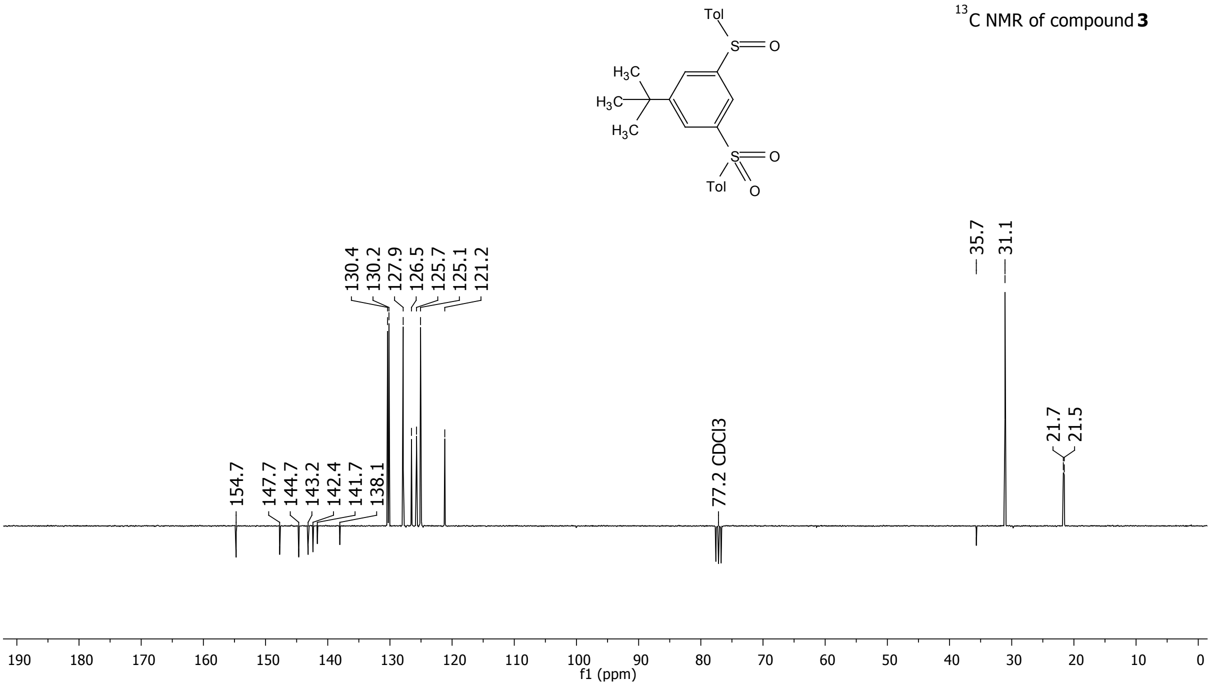

Figure S9. ^{13}C NMR spectrum of compound **3** in CDCl$_3$

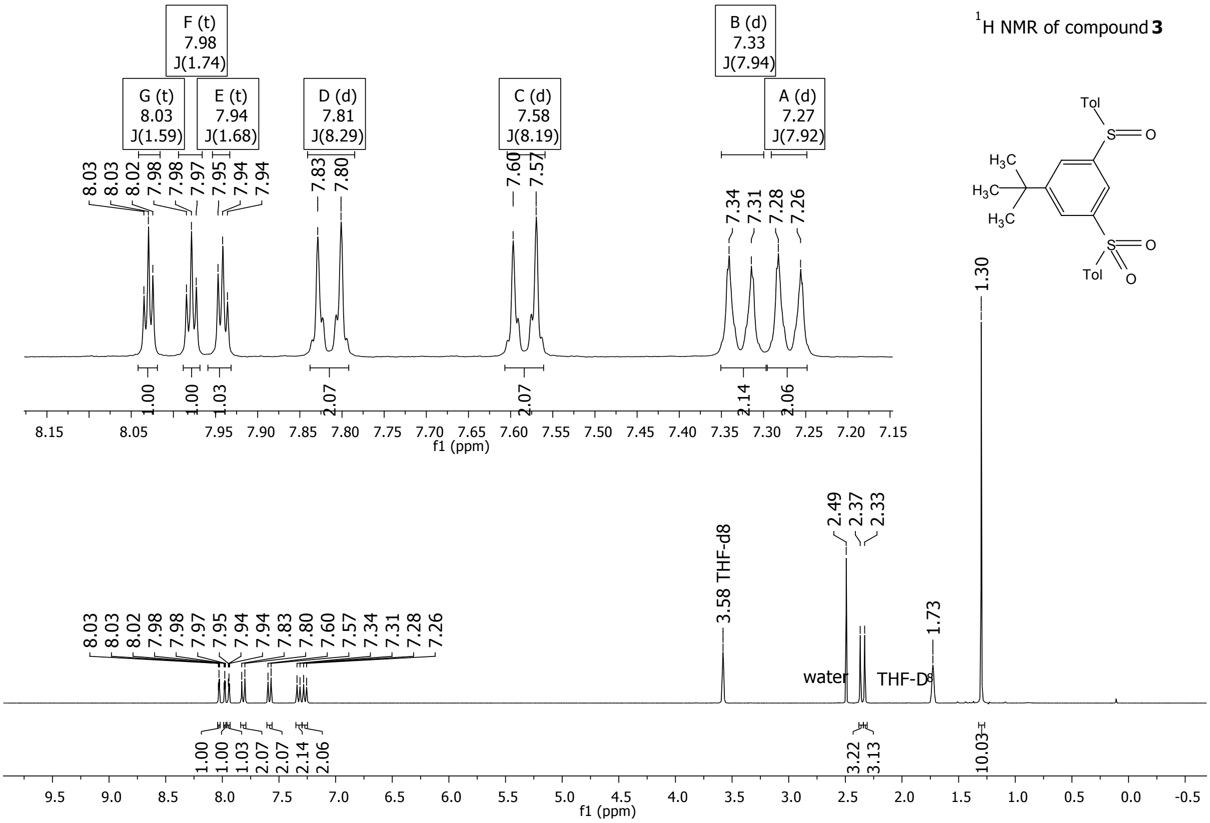

Figure S10. ^{1}H NMR spectrum of compound **3** in THF-D$_8$

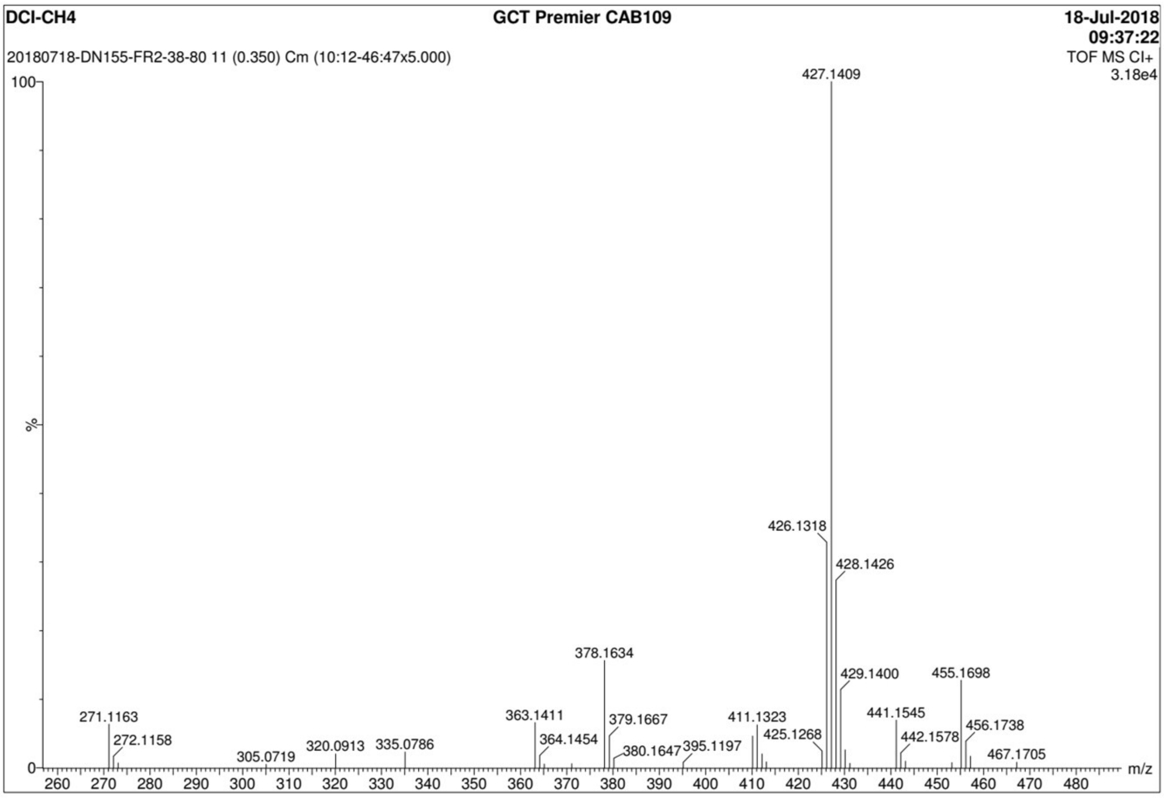

Figure S11. Mass spectrum of compound **3**

HSQC experiment for compound **3**

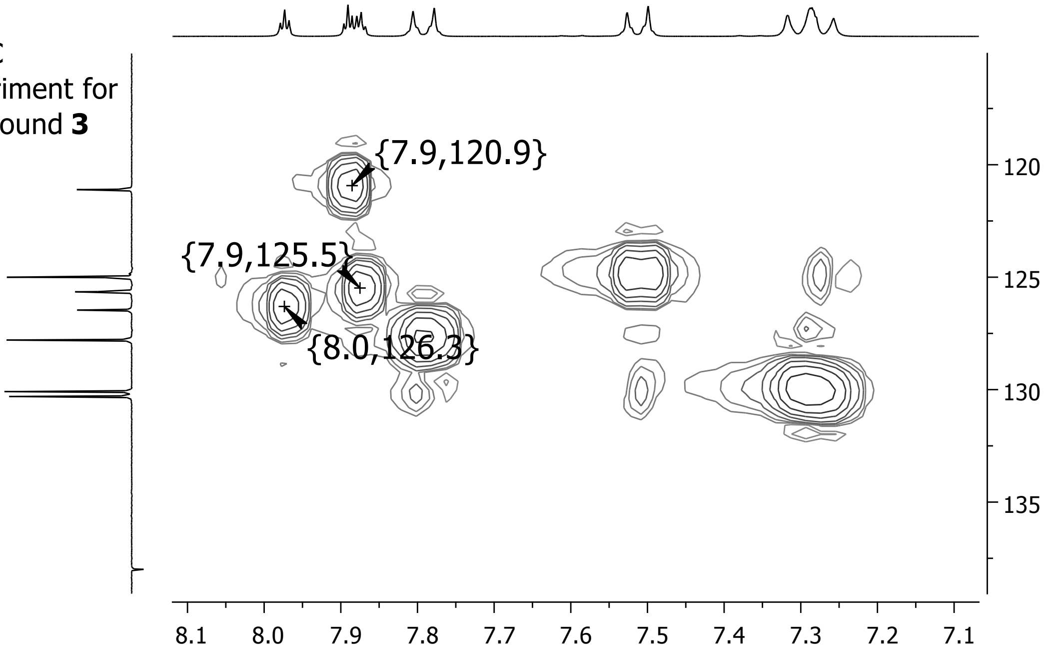

HMBC experiment for compound **3**

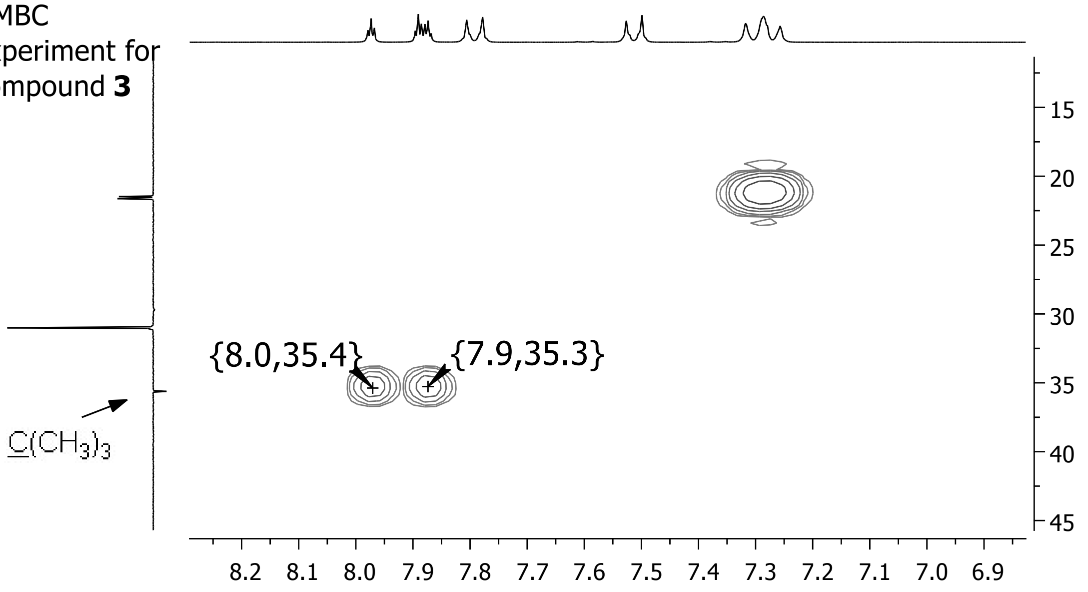

Figure S12. Fragment from the HSQC and HMBC bidimensional NMR experiments for compound **3**

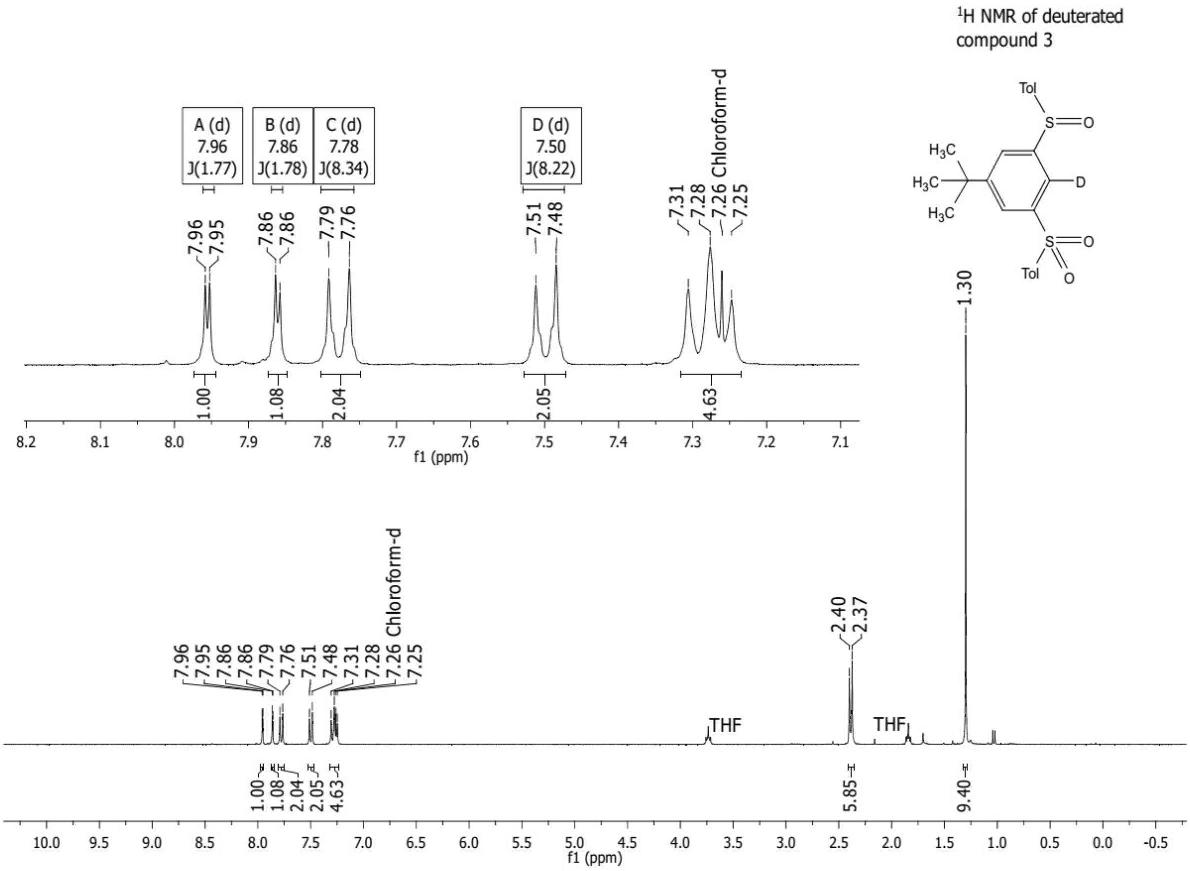

Figure S13. ^{1}H NMR spectrum of deuterated compound **3**

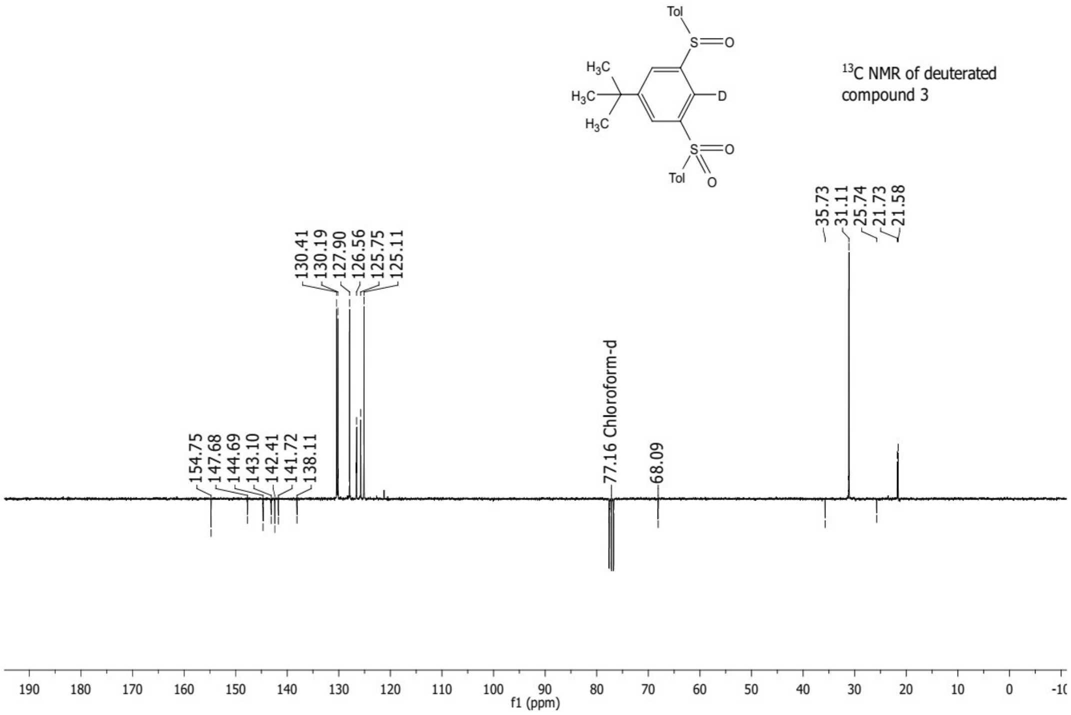

Figure S14. ^{13}C NMR spectrum of deuterated compound **3**

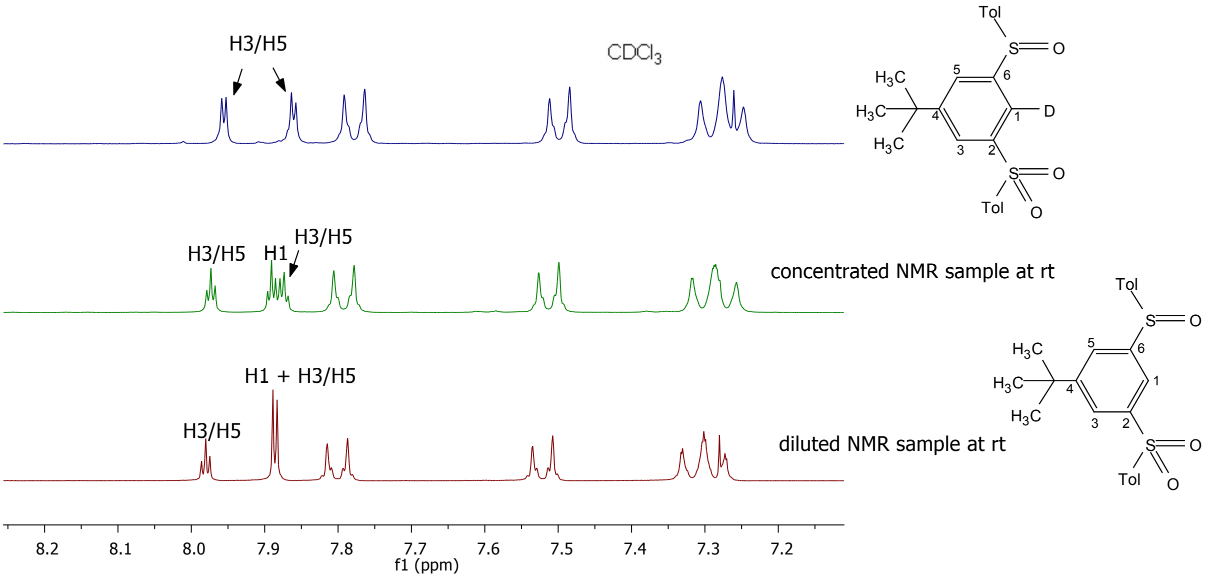

Figure S15. Aromatic region of the 1H NMR spectra of compounds **3** and deuterated compound **3**

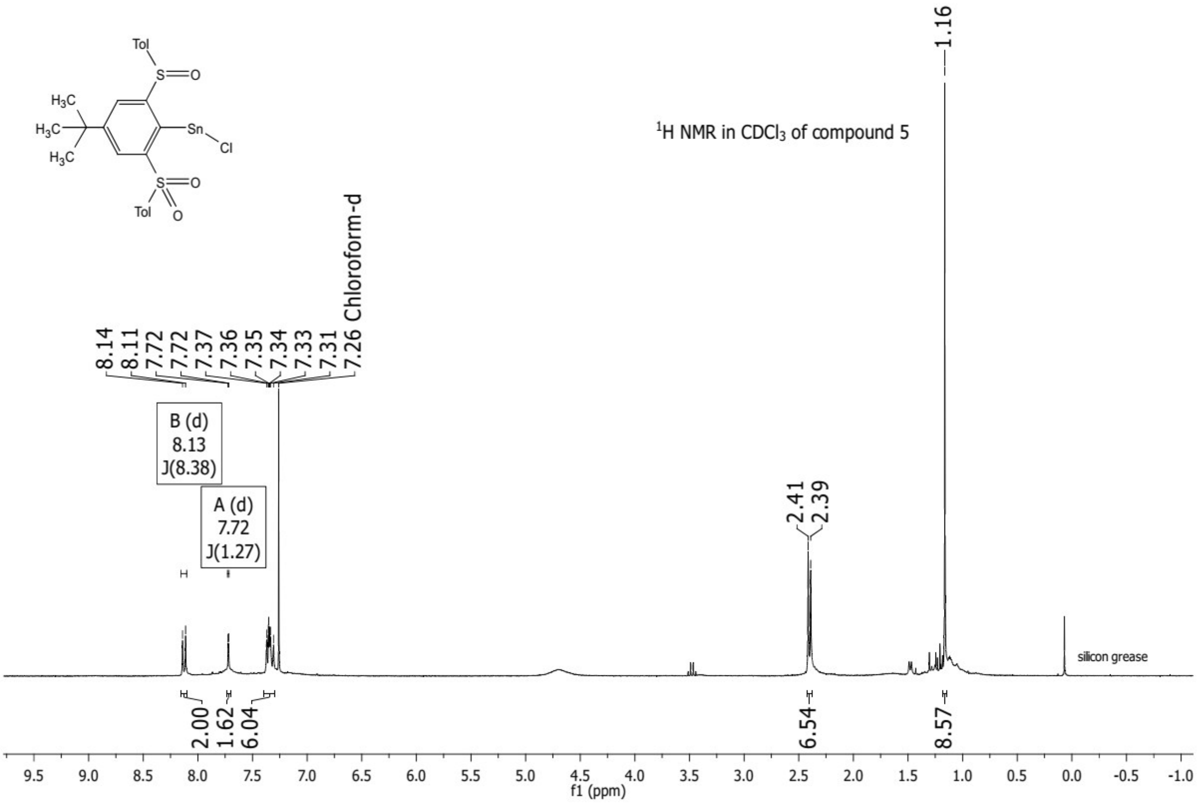

Figure S16. ^{1}H NMR spectrum of compound **5**

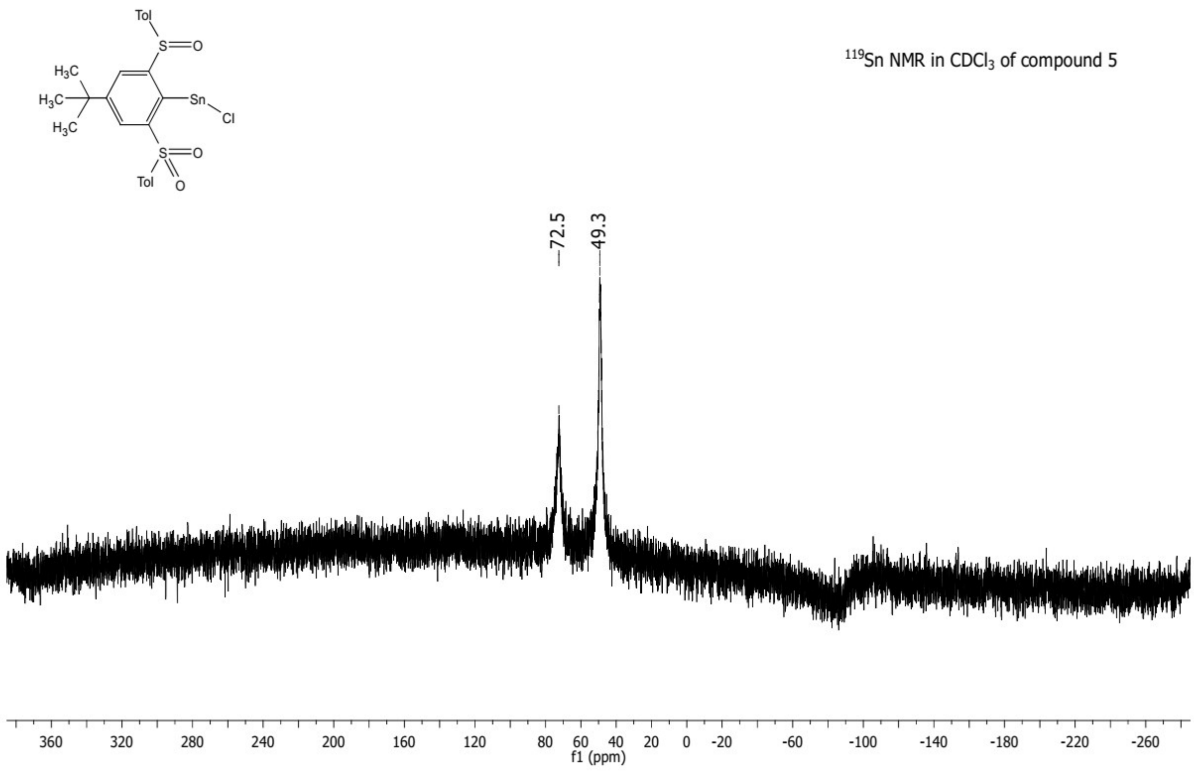

Figure S17. ^{119}Sn NMR spectrum of compound **5** in $CDCl_3$

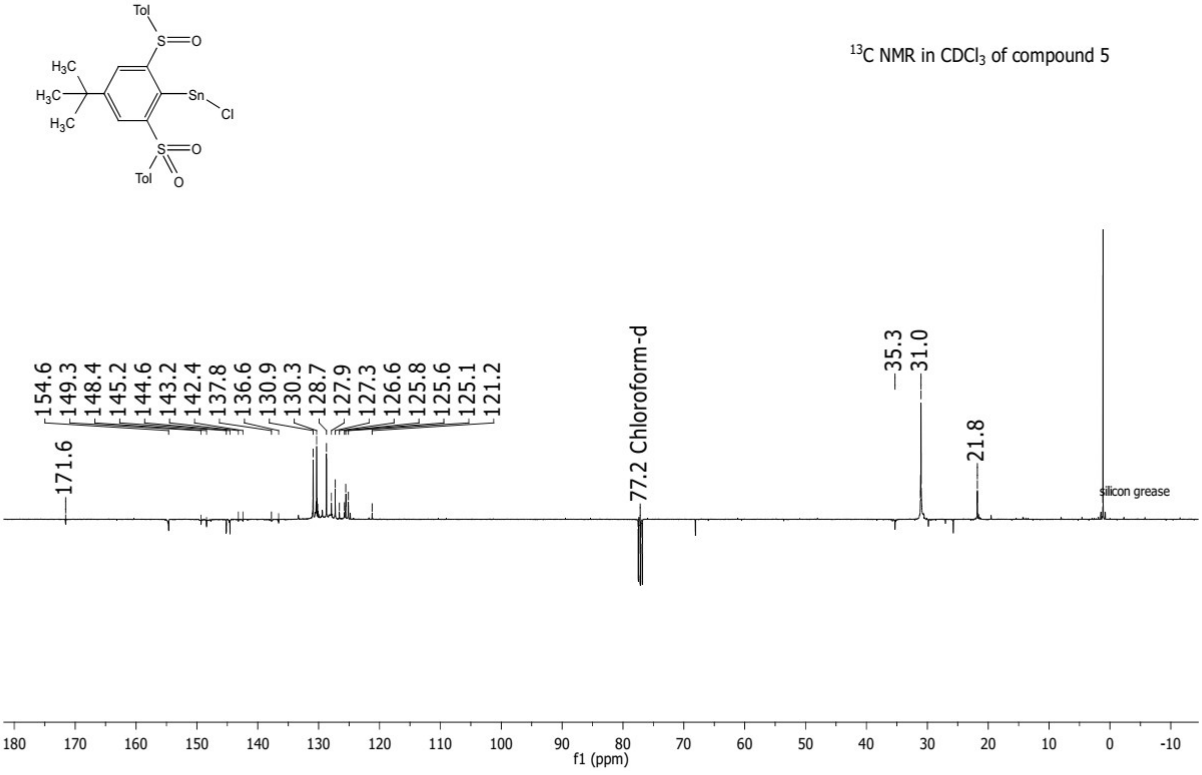

Figure S18. ^{13}C NMR spectrum of compound **5** in $CDCl_3$

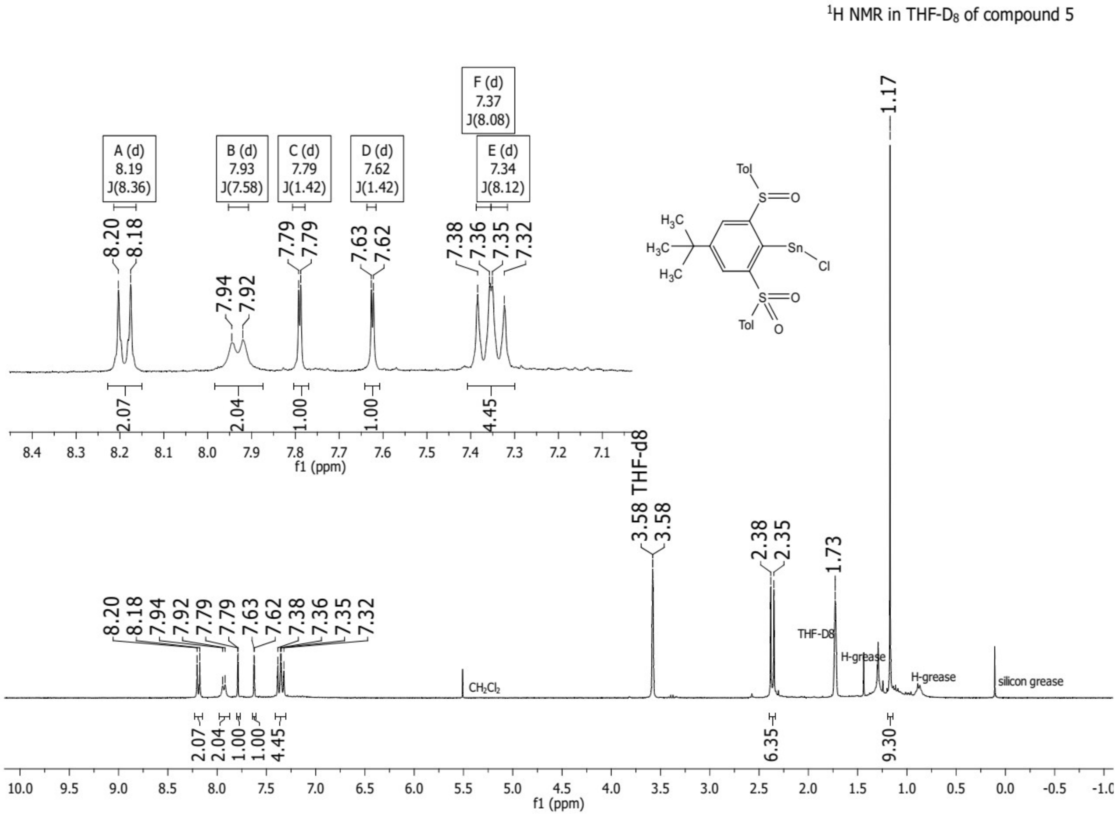

Figure S19. ^{1}H NMR spectrum of compound **5** in THF-D$_8$

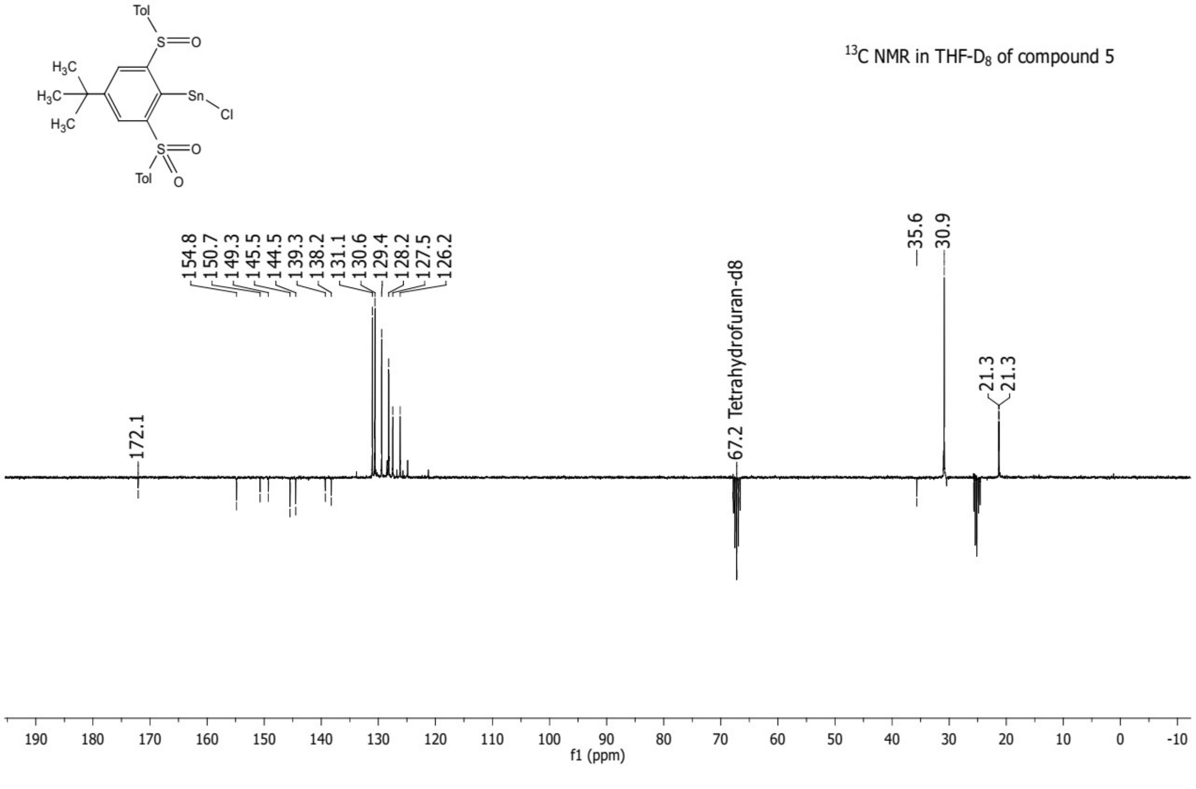

Figure S20. ^{13}C NMR spectrum of compound **5** in THF-D$_8$

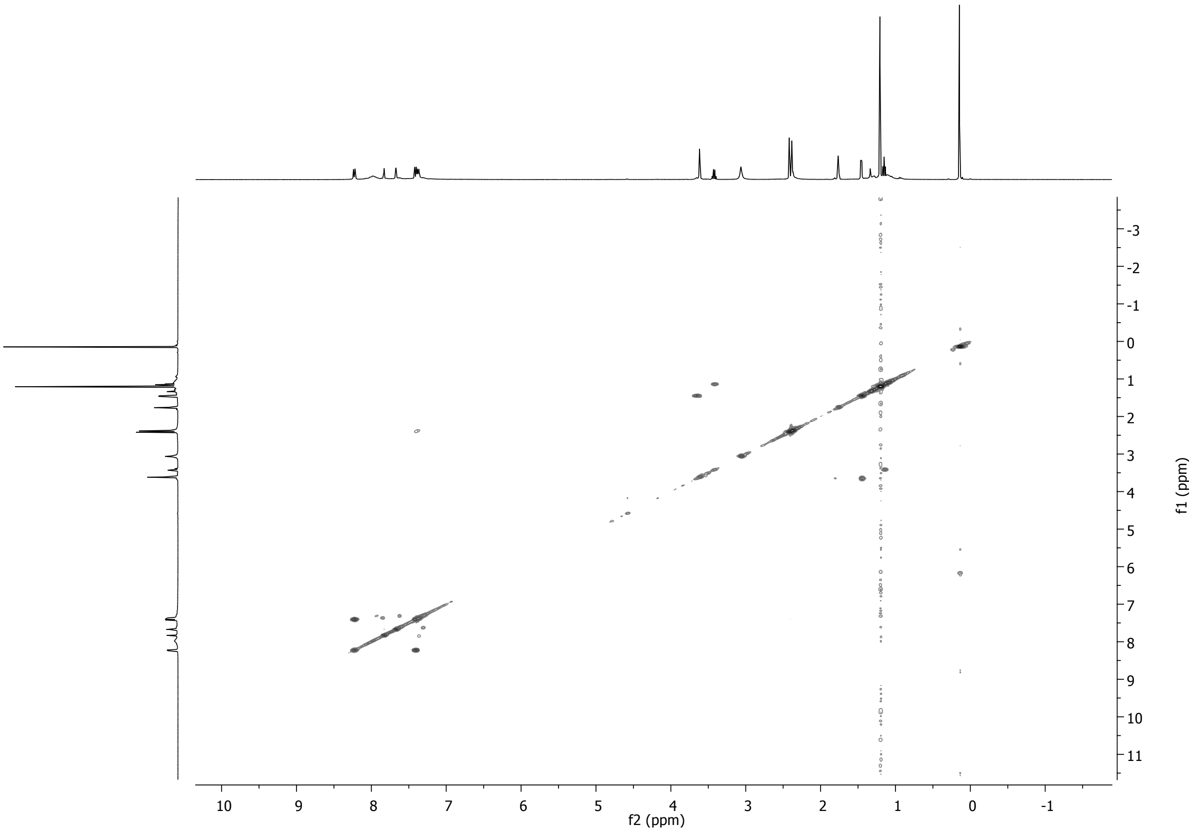

Figure S21. COSY NMR spectrum of compound **5** in THF-D_8

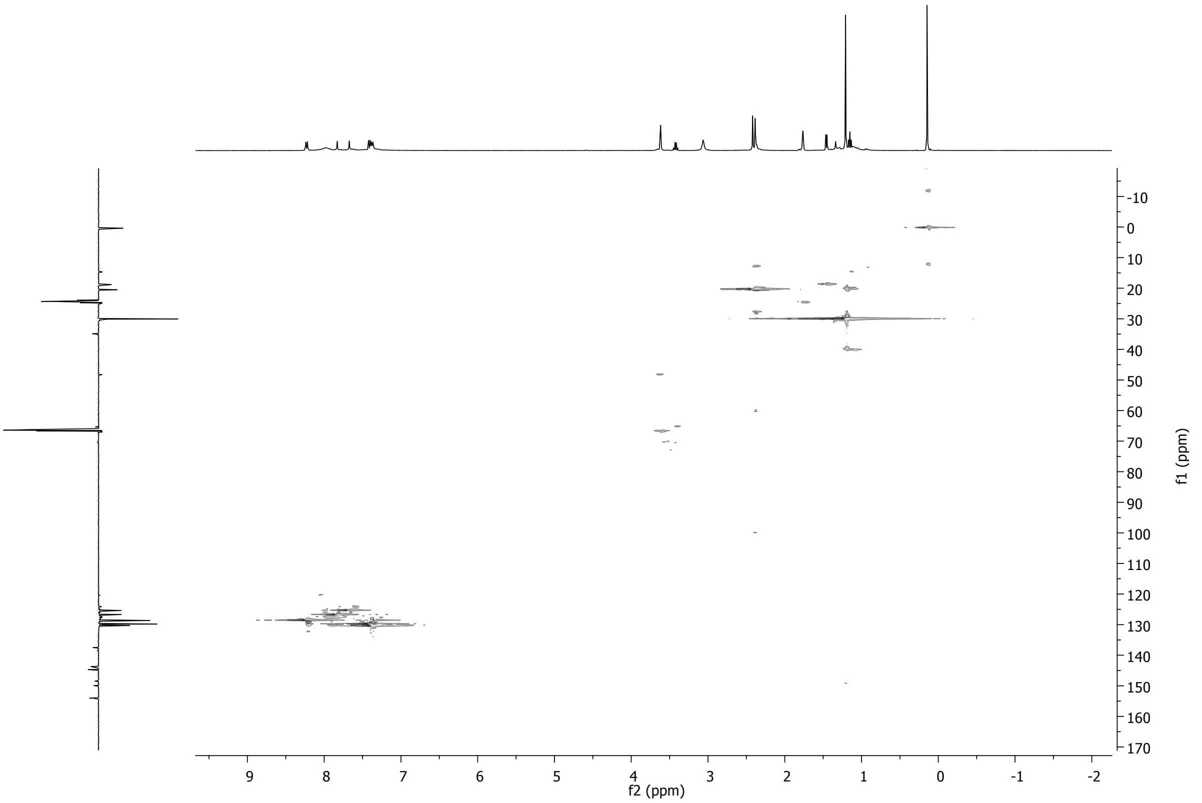

Figure S22. HSQC NMR spectrum of compound 5 in THF-D_8

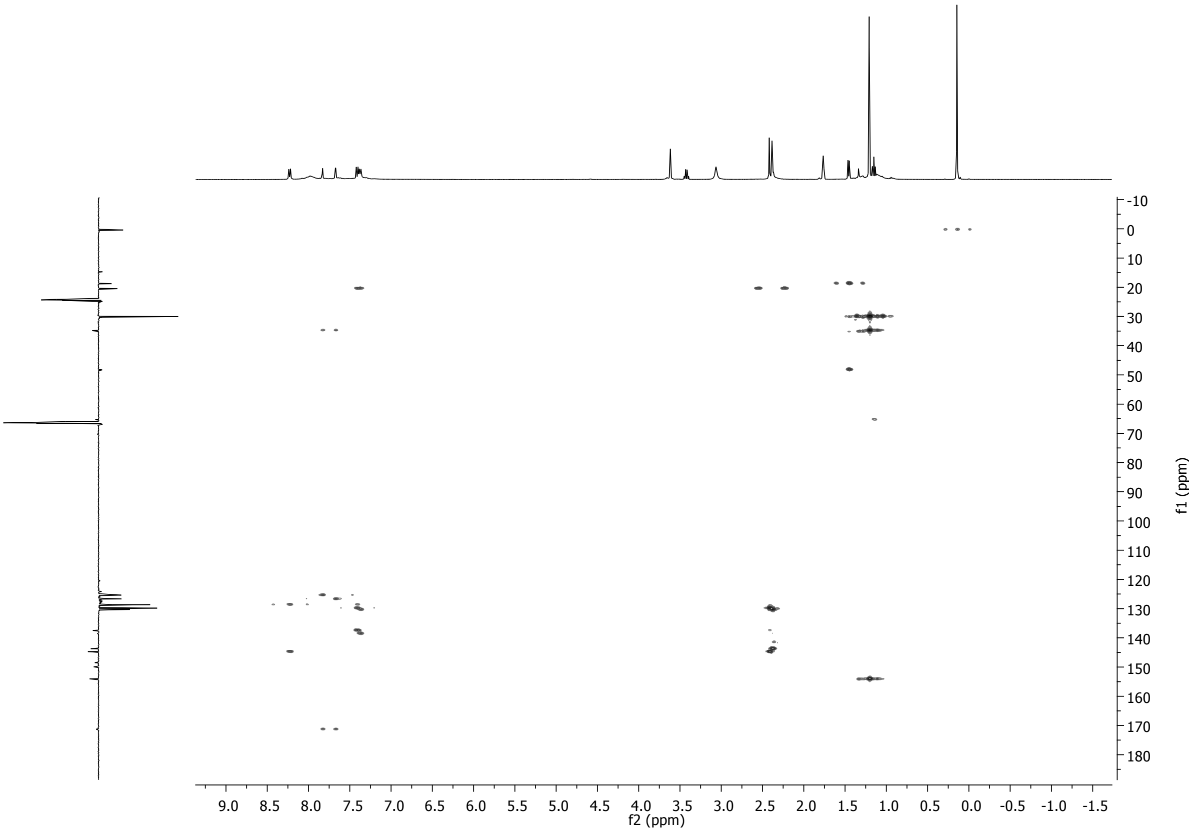

Figure S23. HMBC NMR spectrum of compound **5** in THF-D_8

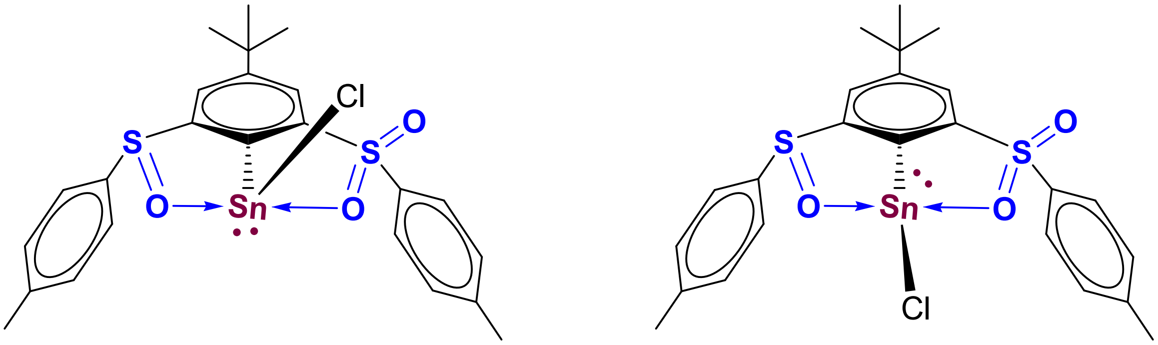

Figure S24. Proposed isomeric structures of stannylene **5**

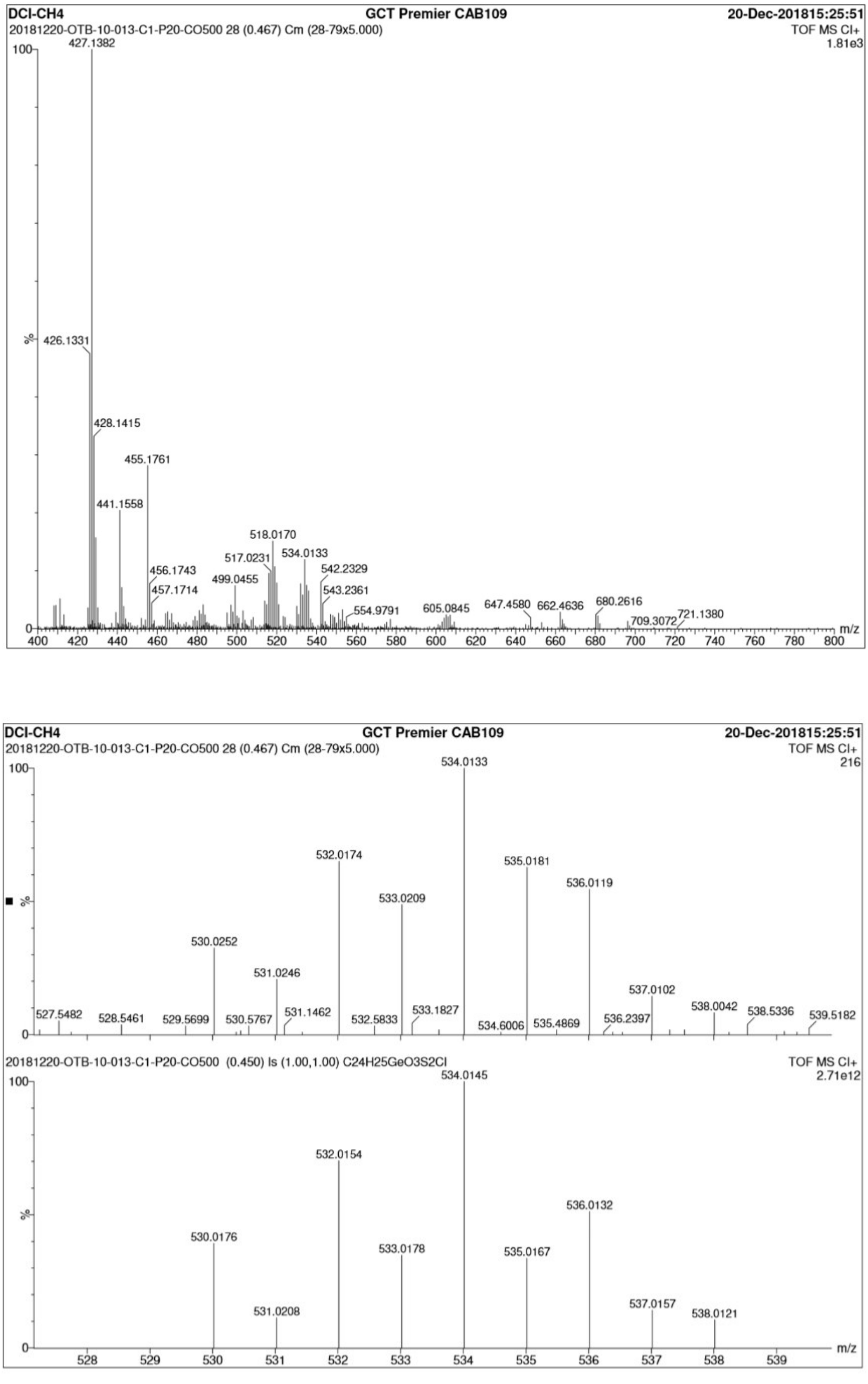

Figure S25. *a)* Mass spectrum of compound **4.** *b)* Mass spectrum of compound **4**, comparison of the theoretical and experimental values of the molecular peak

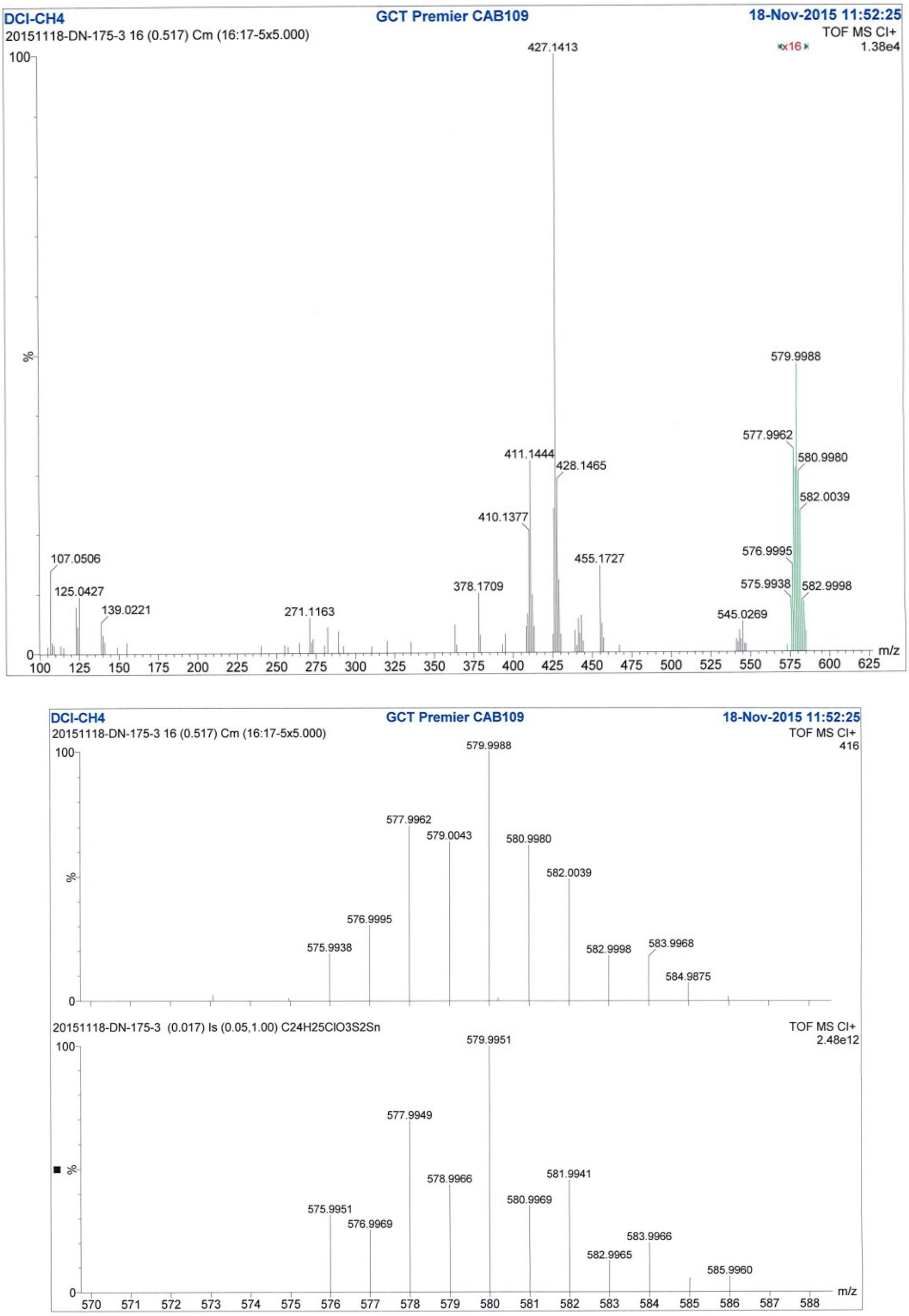

Figure S26. *a)* Mass spectrum of compound **5.** *b)* Mass spectrum of compound **5**, comparison of the theoretical and experimental values of the molecular peak

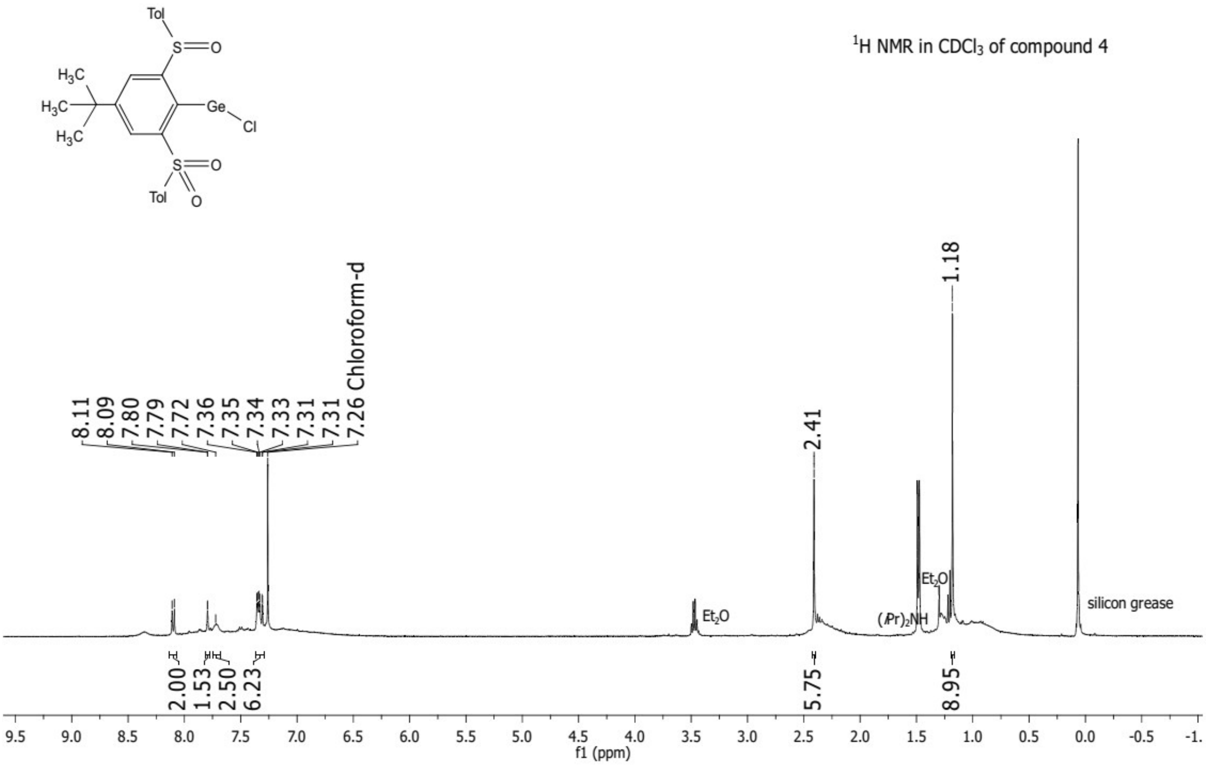

Figure S27. ^{1}H NMR spectrum of compound **4**

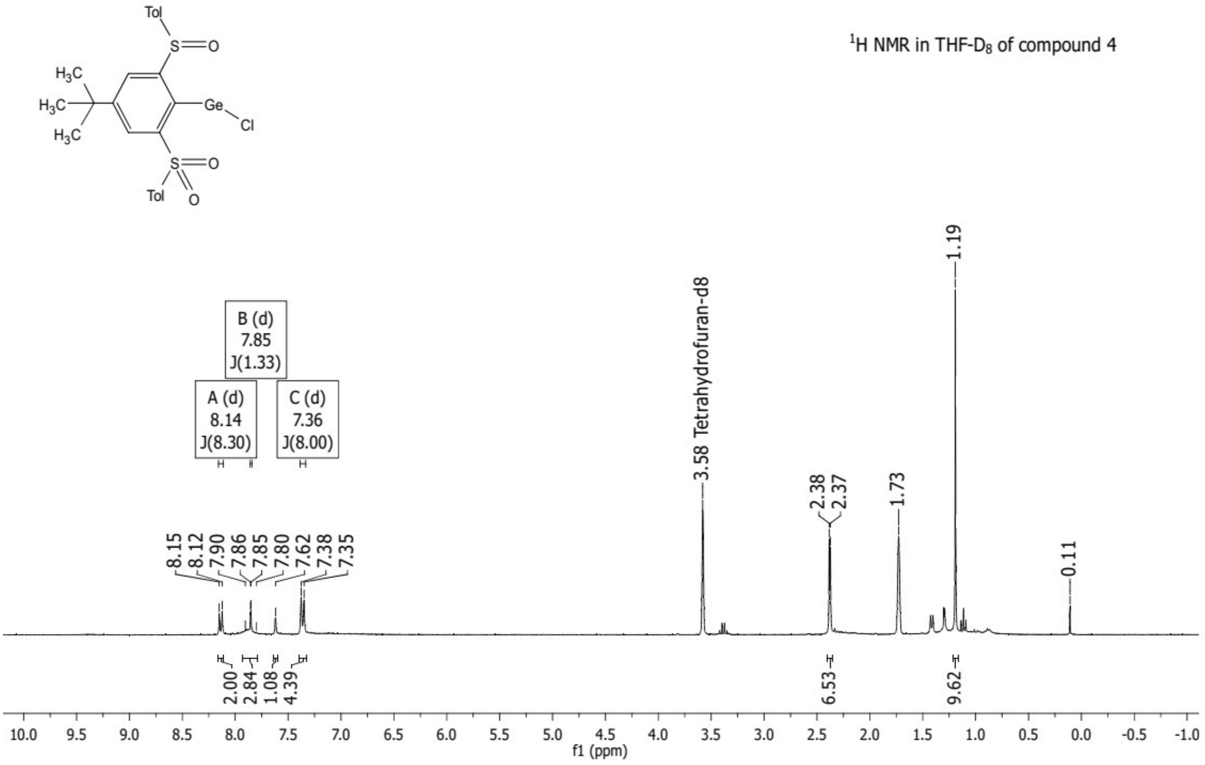

Figure S28. ^{1}H NMR spectrum of compound **4** in THF-D_8

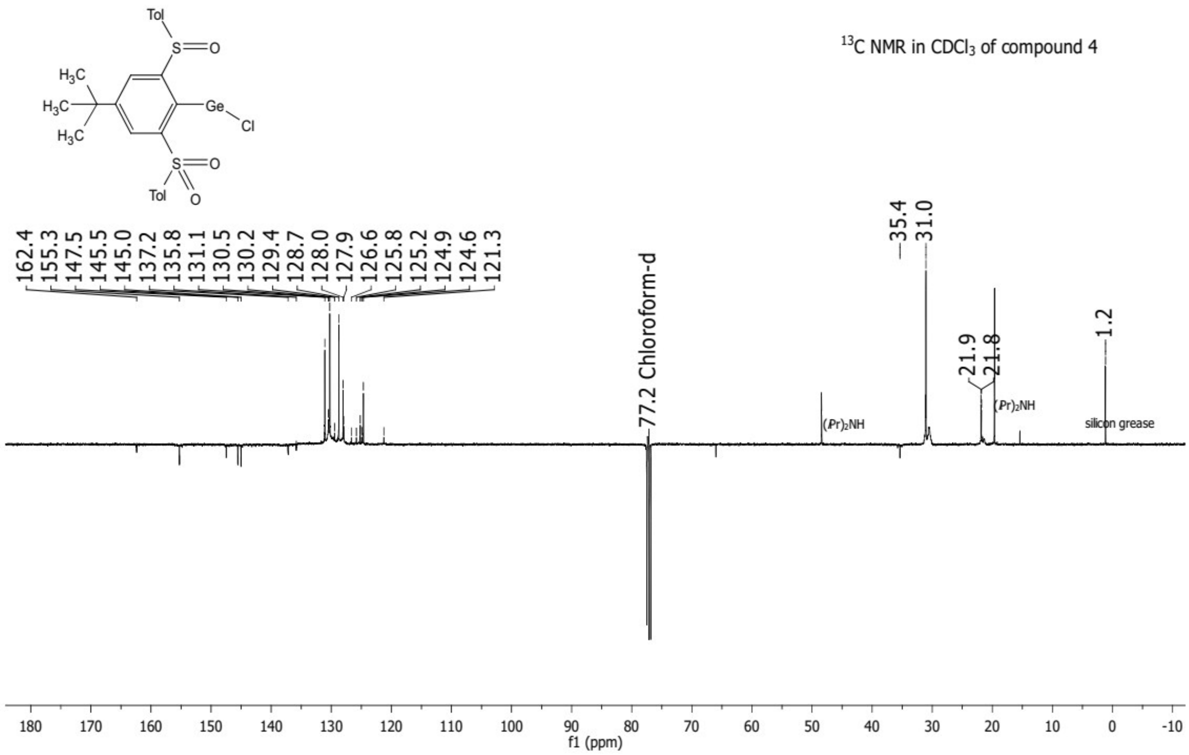

Figure S29. ^{13}C NMR spectrum of compound **4** in $CDCl_3$

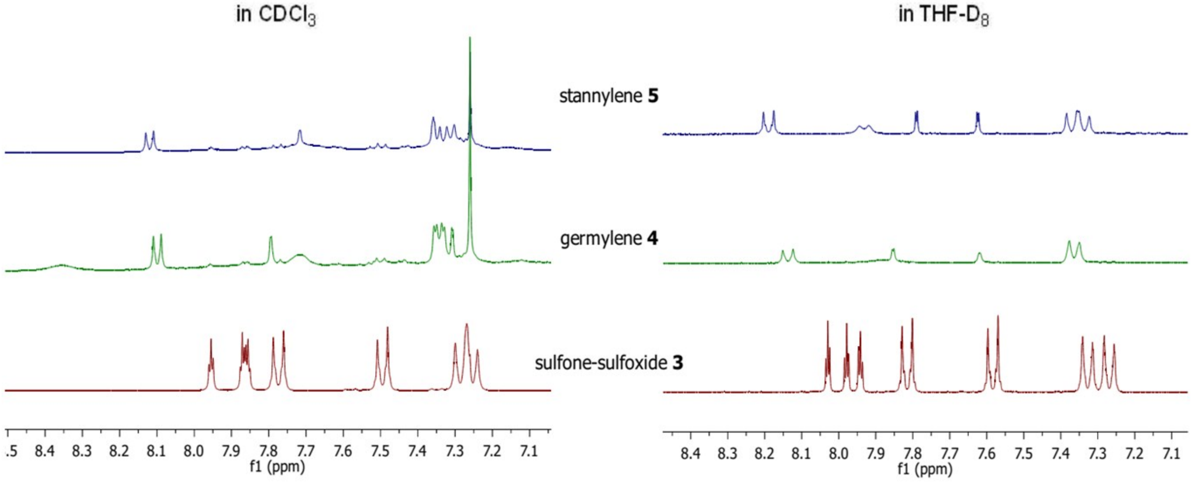

Figure S30. Aromatic region of the ^{1}H NMR spectra in of compounds **3**, **4** and **5** in $CDCl_3$ and THF-D_8

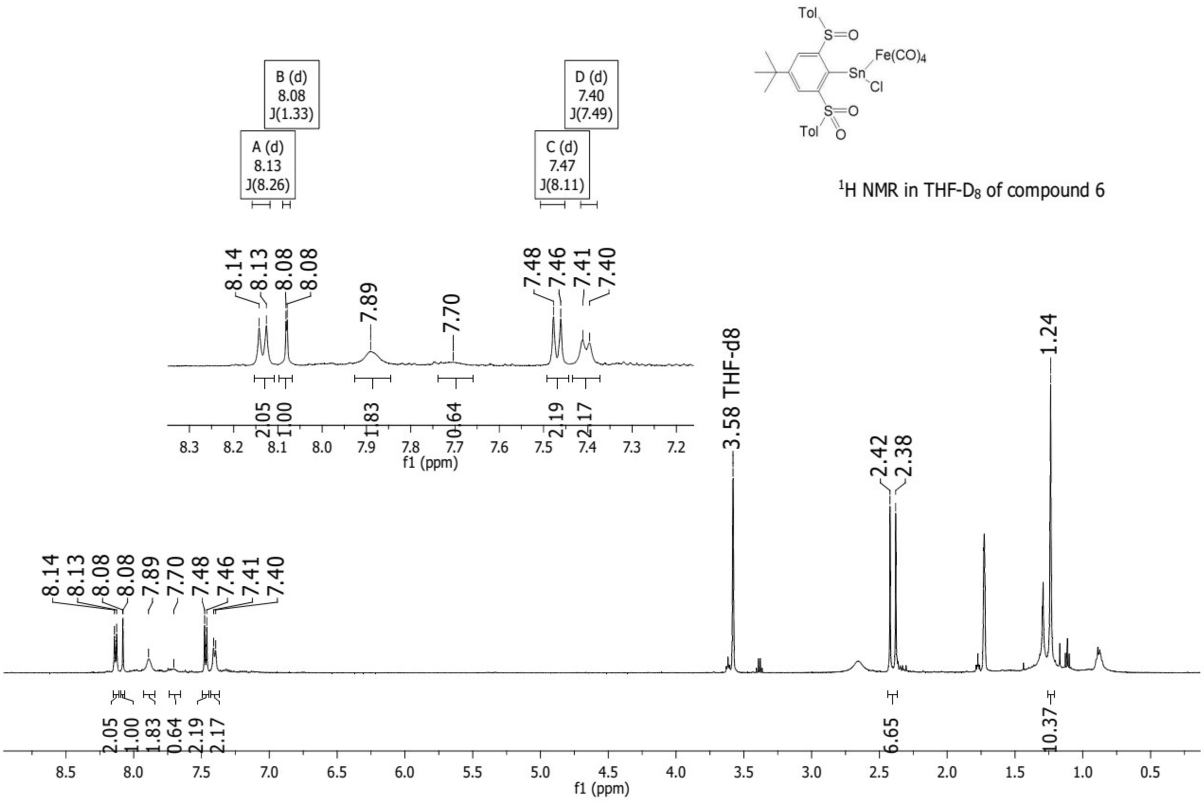

Figure S31. ^{1}H NMR spectrum of compound **6** in THF-D$_8$

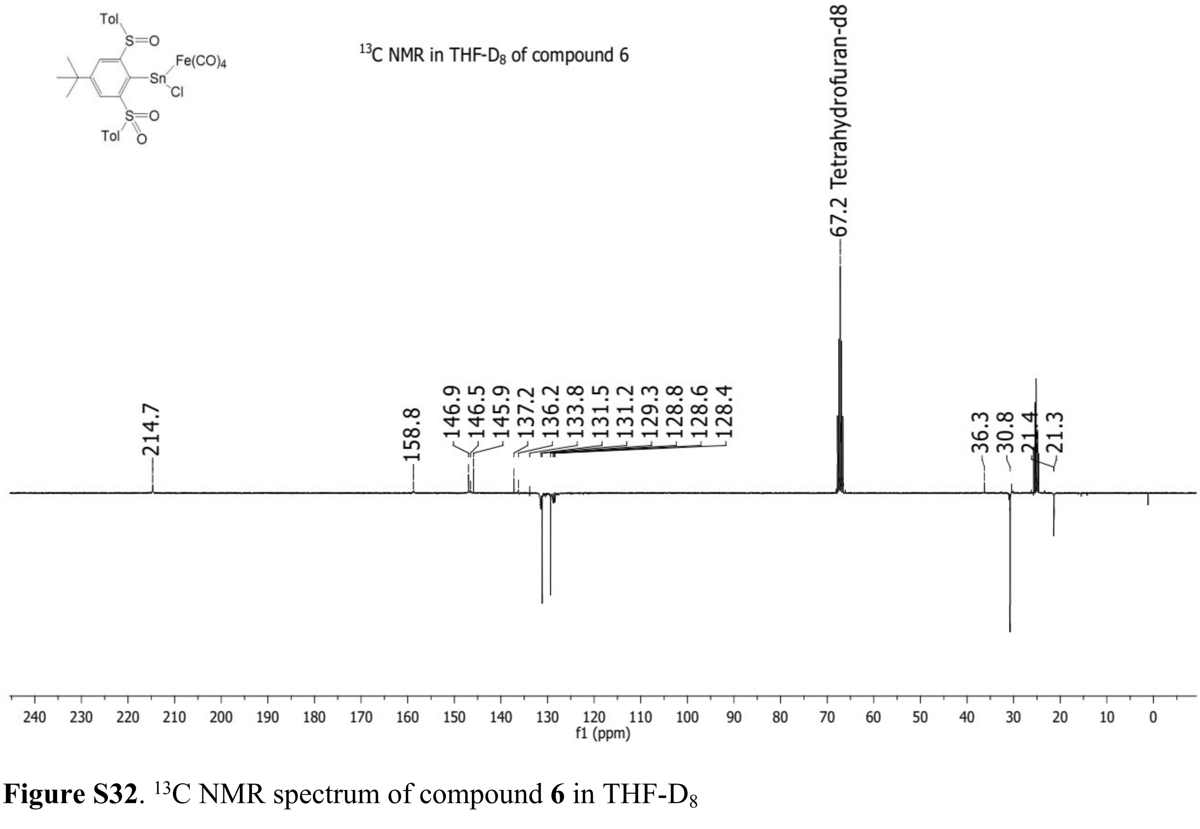

Figure S32. ^{13}C NMR spectrum of compound **6** in THF-D$_8$

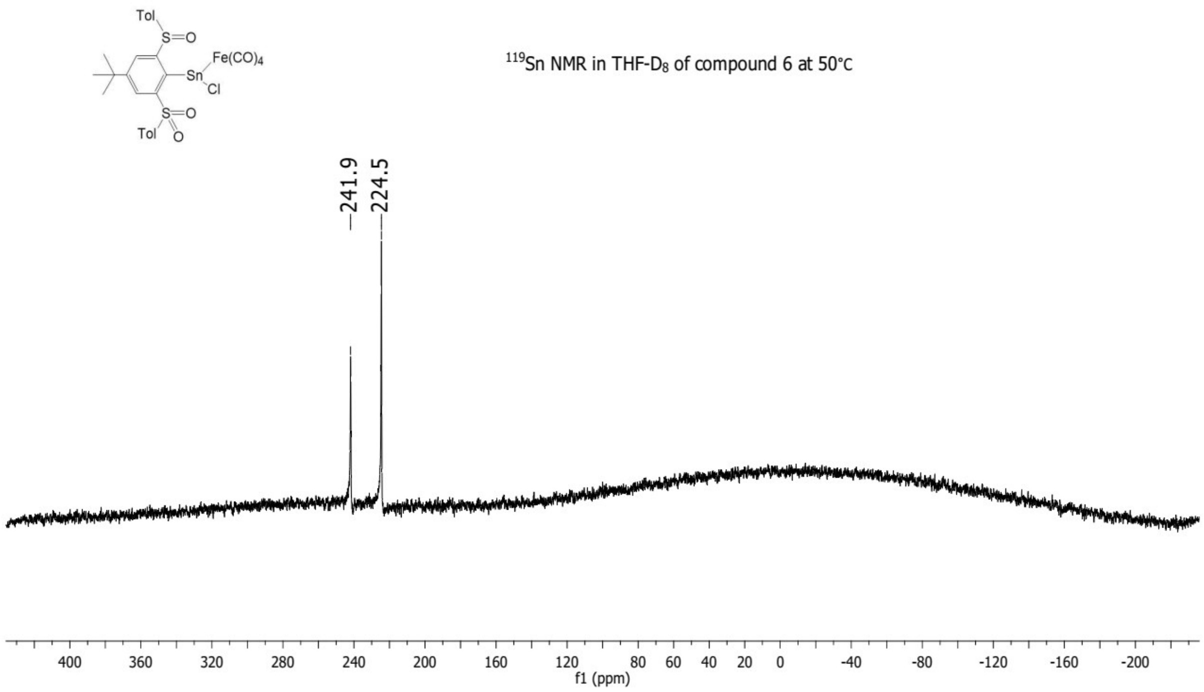

Figure S33. ^{119}Sn NMR spectrum of compound **6** in THF-D$_8$

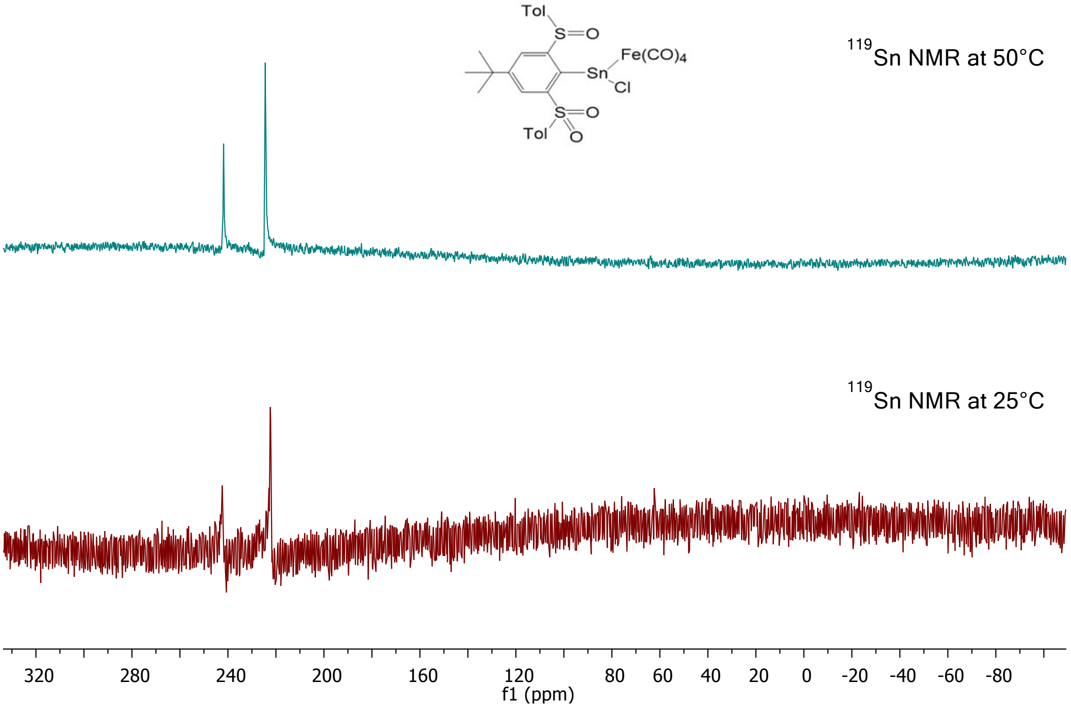

Figure S34. ^{119}Sn NMR spectrum of compound **6** in THF-D$_8$ at 25 and 50 °C

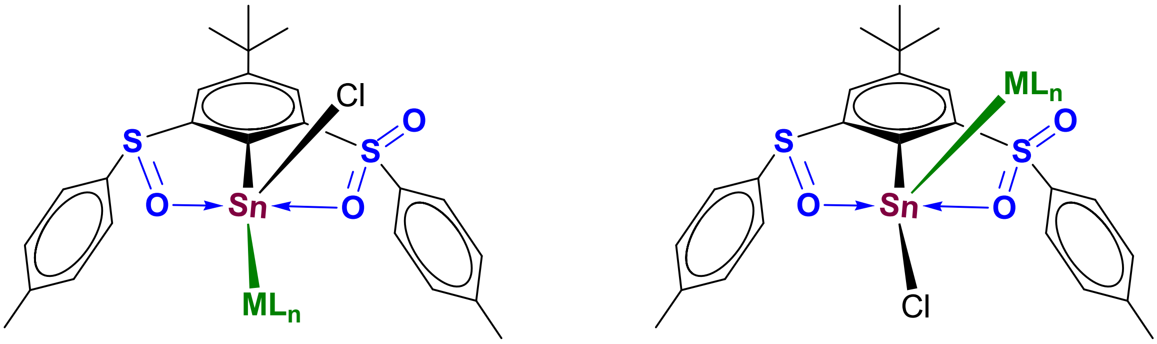

Figure S35. Proposed isomeric structures of stannylene-iron complex **6**

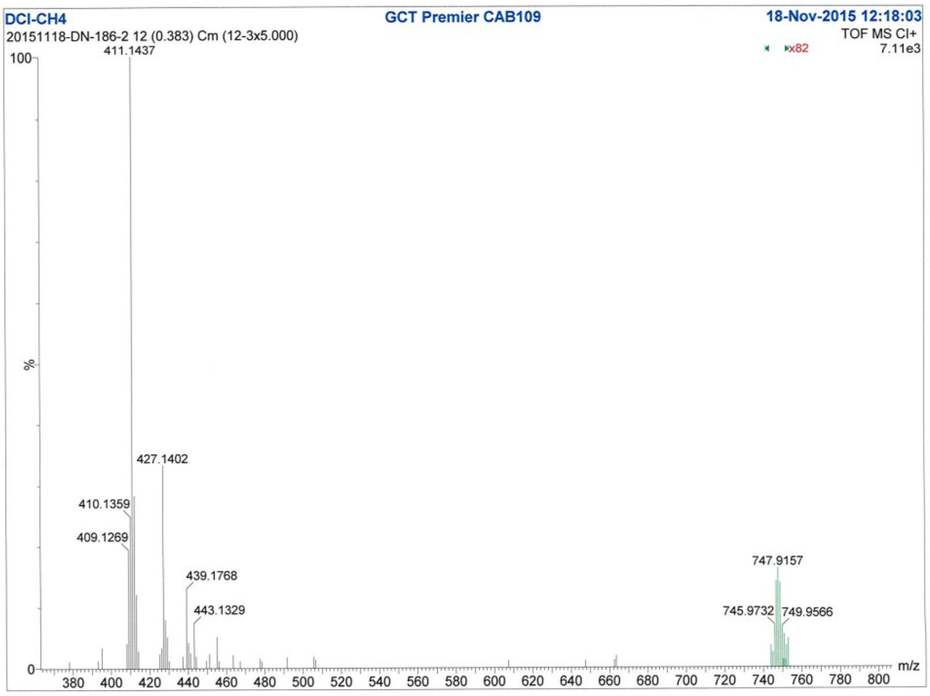

Figure S36. Mass spectrum of compound **6**

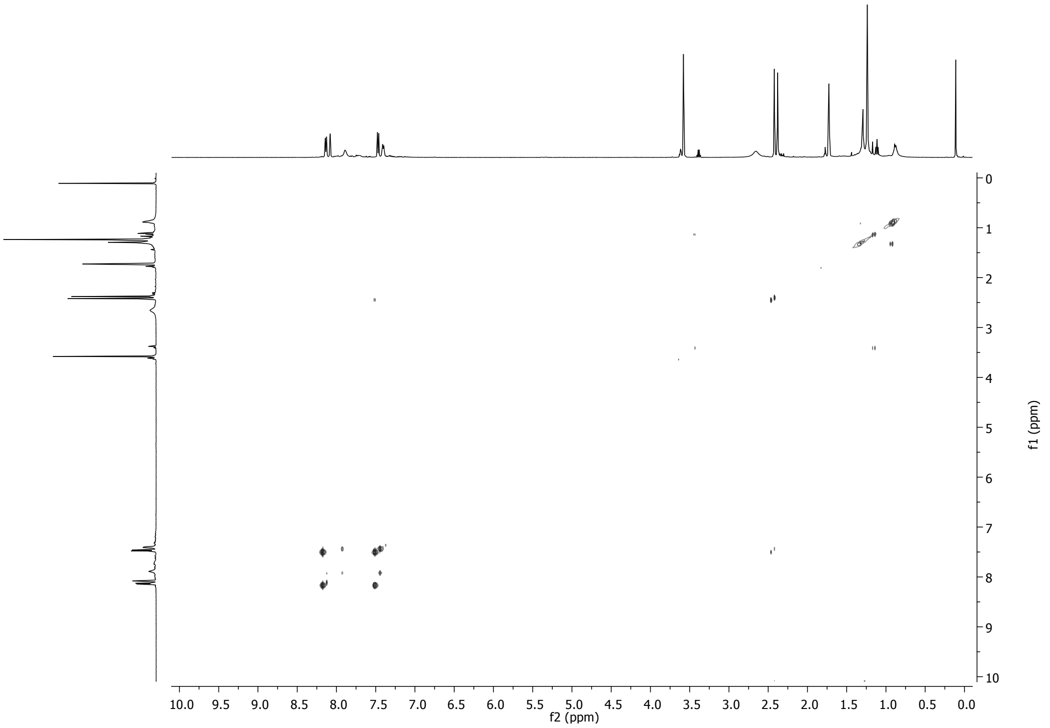

Figure S37. COSY NMR spectrum of compound **6** in THF-D_8

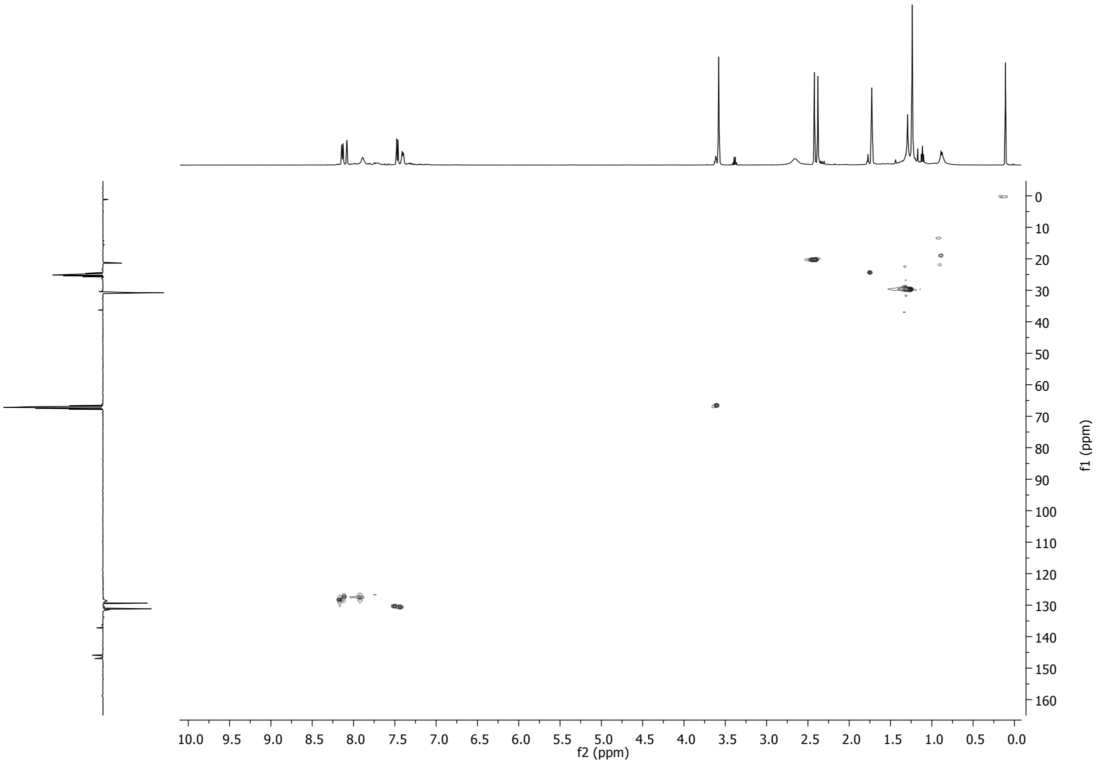

Figure S38. HSQC NMR spectrum of compound **6** in THF-D_8

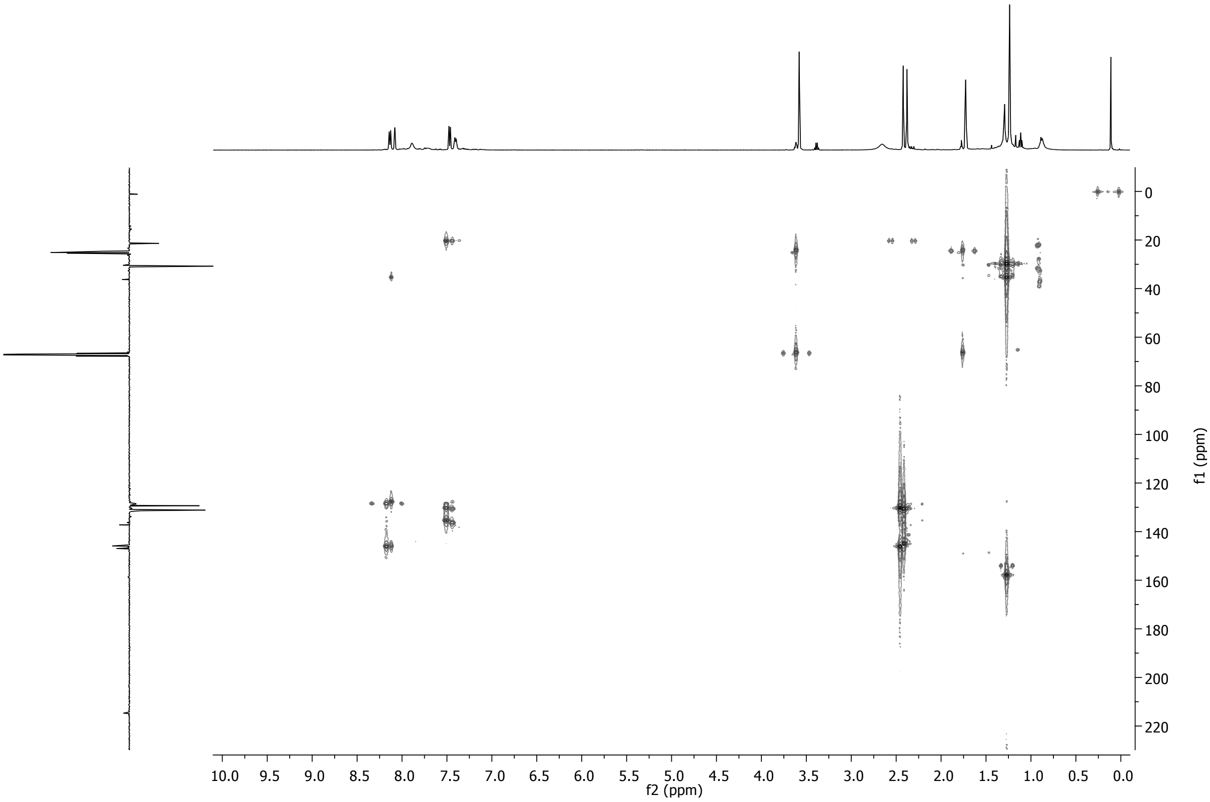

Figure S39. HMBC NMR spectrum of compound **6** in THF-D$_8$

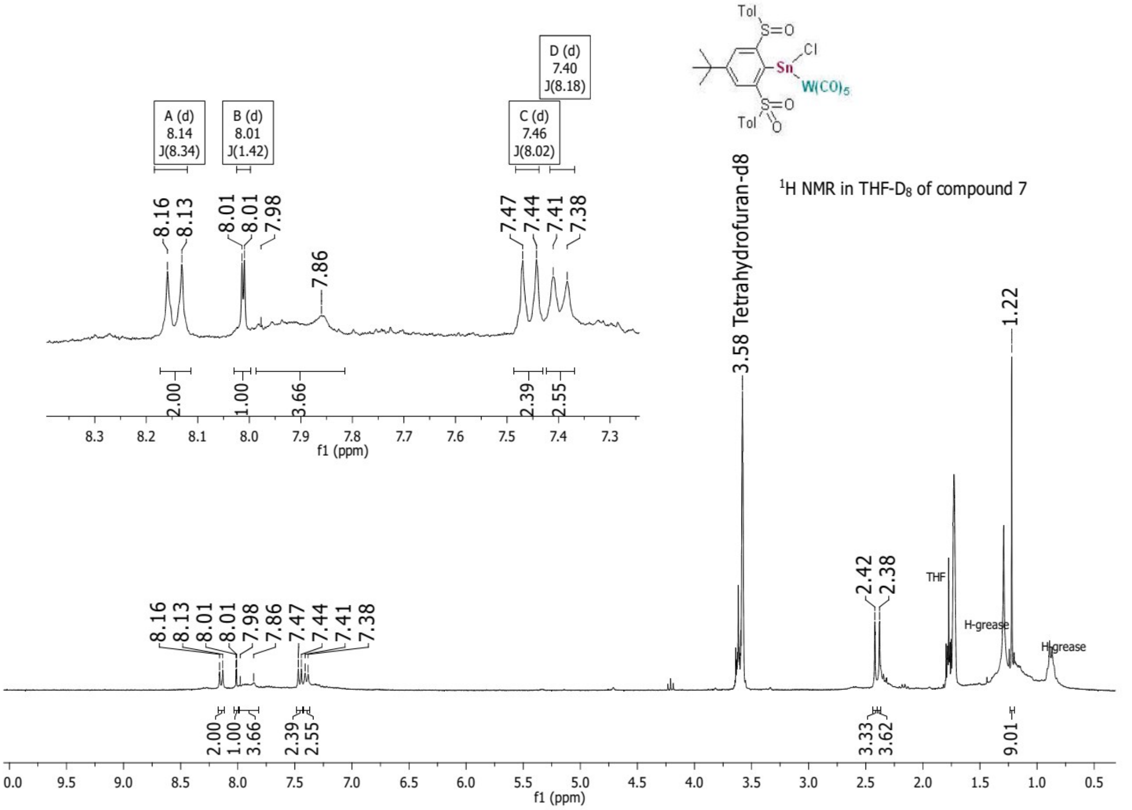

Figure S40. ^{1}H NMR spectrum of compound **7** in THF-D$_8$

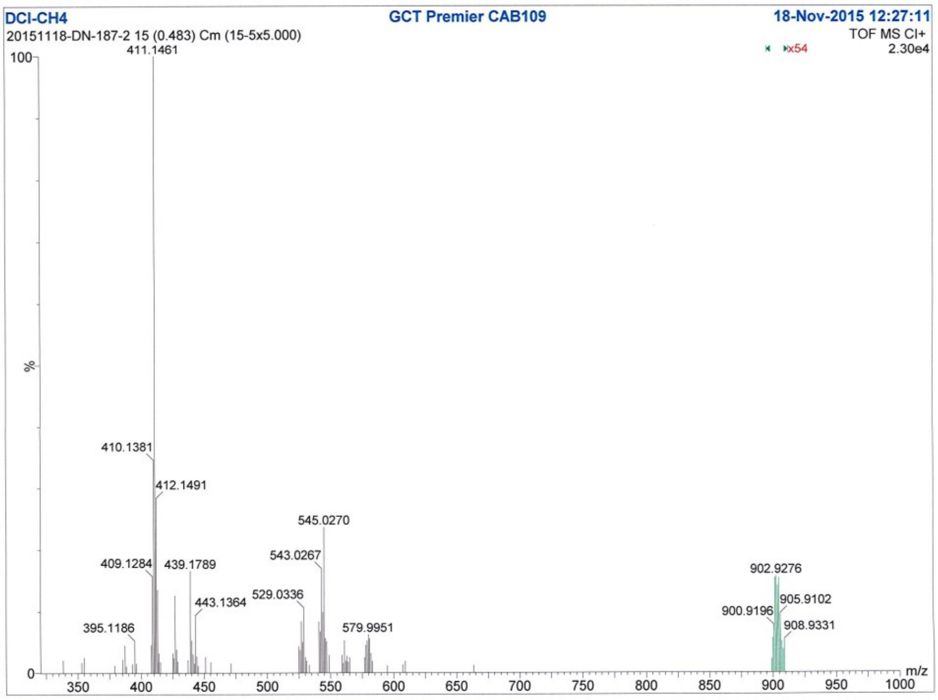

Figure S41.Mass spectrum of compound **7**

Crystallographic data

Table S1. Crystal data and structure refinement for **2**.

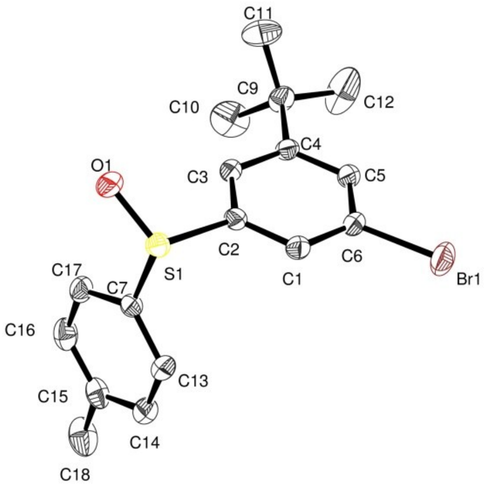

Empirical formula	C17 H19 Br O S	
Formula weight	351.28	
Temperature	193(2) K	
Wavelength	0.71073 A	
Crystal system, space group	monoclinic, $P\ 2_1/c$	
Unit cell dimensions	a = 12.3587(5) A	alpha = 90 deg.
	b = 12.4755(5) A	beta = 107.9286(13) deg.
	c = 11.0104(4) A	gamma = 90 deg.
Volume	1615.16(11) A^3	
Z, Calculated density	4, 1.445 Mg/m^3	
Absorption coefficient	2.668 mm^-1	
F(000)	720	
Crystal size	0.38 x 0.18 x 0.14 mm	
Theta range for data collection	3.27 to 30.54 deg.	
Limiting indices	-17<=h<=17, -17<=k<=17, -15<=l<=14	
Reflections collected / unique	49038 / 4919 [R(int) = 0.0680]	
Completeness to theta = 30.54	99.6 %	
Max. and min. transmission	0.7461 and 0.5813	
Refinement method	Full-matrix least-squares on F^2	
Data / restraints / parameters	4919 / 0 / 185	
Goodness-of-fit on F^2	0.916	
Final R indices [I>2sigma(I)]	R1 = 0.0364, wR2 = 0.1089	
R indices (all data)	R1 = 0.0570, wR2 = 0.1256	
Largest diff. peak and hole	0.816 and -0.966 e.A^-3	

Table S2. Crystal data and structure refinement for **3**.

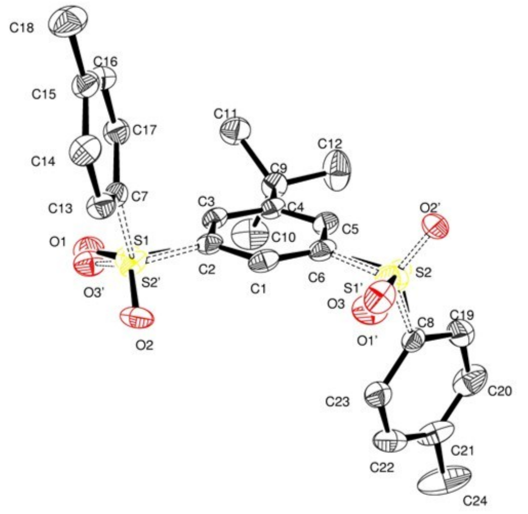

Empirical formula	C24 H26 O3 S2
Formula weight	426.57
Temperature	193(2) K
Wavelength	0.71073 A
Crystal system, space group	Triclinic, P□1
Unit cell dimensions	a = 9.035(4) A alpha = 100.829(17) deg.
	b = 9.959(4) A beta = 101.45(3) deg.
	c = 13.309(10) A gamma = 102.442(15) deg.
Volume	1112.4(11) A^3
Z, Calculated density	2, 1.273 Mg/m^3
Absorption coefficient	0.261 mm^-1
Max. and min. transmission	0.7457 and 0.7052
F(000)	452
Crystal size	0.18 x 0.12 x 0.04 mm
Theta range for data collection	5.142 to 26.367 deg.
Limiting indices	-11<=h<=11, -12<=k<=12, -15<=l<=16
Reflections collected / unique	17659 / 4475 [R(int) = 0.0255]
Completeness to theta = 25.242	98.3 %
Refinement method	Full-matrix least-squares on F^2
Data / restraints / parameters	4475 / 109 / 314
Goodness-of-fit on F^2	1.12
Final R indices [I>2sigma(I)]	R1 = 0.0475, wR2 = 0.1095
R indices (all data)	R1 = 0.0553, wR2 = 0.1129

In the crystal, the compound has crystallized according two orientations, one containing the atoms S1, O1, O2, S2 and O3 (with an occupancy of 0.63) and another one with S1', O1', O2', S2' and O3' (with an occupancy of 0.37). Only the bond lengths and the bond angles of the structure with an occupancy of 0.63 are discussed.

Table S3. Crystal data and structure refinement for **4**.

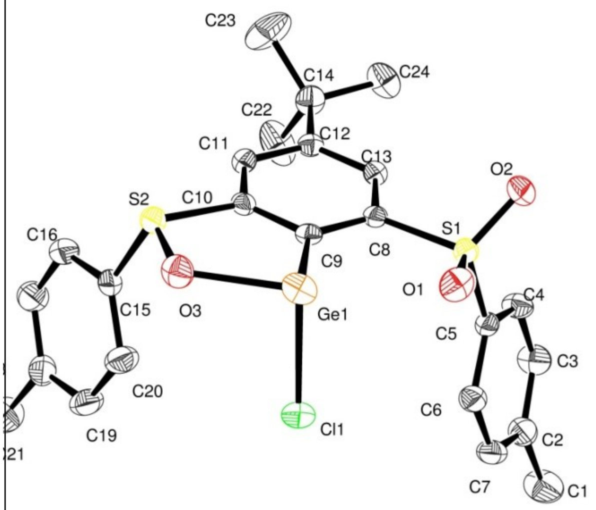

Empirical formula	C24 H25 Cl Ge O3 S2
Formula weight	533.62
Temperature	193(2) K
Wavelength	0.71073 A
Crystal system, space group	Triclinic, $P\bar{1}$
Unit cell dimensions	a = 9.4696(7) A alpha = 105.093(2) deg. b = 9.6861(7) A beta = 90.070(2) deg. c = 13.7730(10) A gamma = 94.398(2) deg.
Volume	1215.84(15) A^3
Z, Calculated density	2, 1.458 Mg/m^3
Absorption coefficient	1.565 mm^-1
F(000)	548
Crystal size	0.200 x 0.160 x 0.160 mm
Theta range for data collection	5.125 to 29.574 deg.
Limiting indices	-13<=h<=13, -13<=k<=13, -19<=l<=19
Reflections collected / unique	42232 / 6785 [R(int) = 0.0325]
Completeness to theta = 25.242	99.0 %
Max. and min. transmission	0.7463 and 0.7100
Refinement method	Full-matrix least-squares on F^2
Data / restraints / parameters	6785 / 0 / 285
Goodness-of-fit on F^2	1.047
Final R indices [I>2sigma(I)]	R1 = 0.0333, wR2 = 0.0829
R indices (all data)	R1 = 0.0444, wR2 = 0.0883
Largest diff. peak and hole	1.063 and -0.412 e.A^-3

Table S4. Crystal data and structure refinement for **5**.

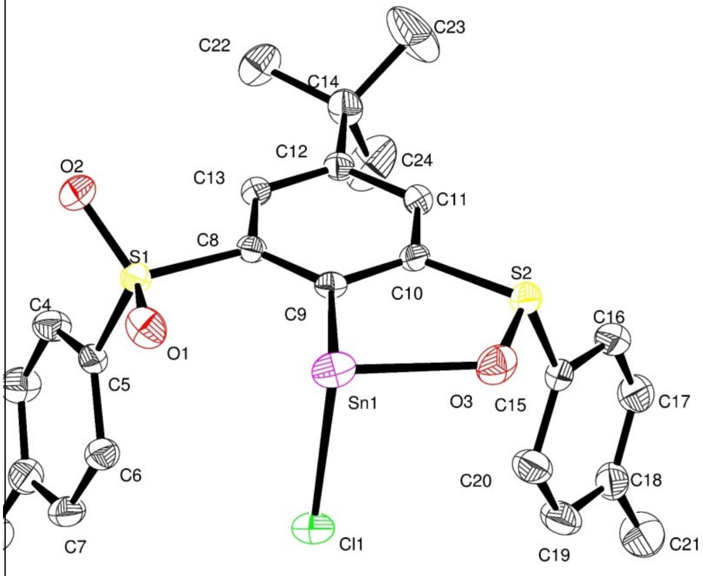

Empirical formula	C24 H25 Cl O3 S2 Sn
Formula weight	579.72
Temperature	193(2) K
Wavelength	0.71073 A
Crystal system, space group	Triclinic, P□1
Unit cell dimensions	a = 9.5483(7) A alpha = 75.257(2) deg.
	b = 9.7909(7) A beta = 89.804(2) deg.
	c = 13.8355(10) A gamma = 84.233(3) deg.
Volume	1244.19(16) A^3
Z, Calculated density	2, 1.547 Mg/m^3
Absorption coefficient	1.325 mm^-1
Max. and min. transmission	0.7466 and 0.7043
F(000)	584
Crystal size	0.160 x 0.140 x 0.140 mm
Theta range for data collection	2.946 to 33.782 deg.
Limiting indices	-14<=h<=14, -15<=k<=12, -21<=l<=21
Reflections collected / unique	35803 / 9960 [R(int) = 0.0298]
Completeness to theta = 25.242	99.7 %
Refinement method	Full-matrix least-squares on F^2
Data / restraints / parameters	9960 / 0 / 285
Goodness-of-fit on F^2	1.029
Final R indices [I>2sigma(I)]	R1 = 0.0300, wR2 = 0.0633
R indices (all data)	R1 = 0.0438, wR2 = 0.0684
Largest diff. peak and hole	0.800 and -0.581 e.A^-3

DFT Calculations

DFT calculations were performed on the pincer ligand **3**, germylene **4** and stannylene **5**. For ligand **3**, four isomers were assessed: two *trans* (**3_I** and **3_II**) and two *cis* (**3_III** and **3_IV**), with two different orientations of the oxygen atom within the sulfoxide unit for each *cis*/*trans* isomer (Figure S42). Calculations were performed both in gaseous phase and solvent (toluene, THF and acetone), as chemical reactions were performed in toluene and THF, while acetone represents the crystallization solvent. In all cases, calculated energies among isomers **3_I-3_IV** are low, the maximum gap being of only 1.7 kcal mol^{-1} (Table S5). Additionally, previous calculation carried out on similar bis-sulfone ligands[1] revealed that rotation barriers are very low (about 1.6 kcal mol^{-1} the calculated activation energies) for these species. Thus, the small energy differences between isomers along with the barrierless *cis-trans* transformation point out the adjustable rotameric behaviour of these pincer ligands. For germylene **4** and stannylene **5** eight isomers were considered in both cases (Figures S43 and S44). Calculations were carried out for these species in gaseous phase, toluene and THF. The calculated energies revel that the most stable isomers within their series are **4_I** and **5_I**, even though the energy differences between species **4_I-4_IV** and **5_I-5_IV** respectively, are very low (see Tables S6 and S7). Yet, the molecular geometries of **4_I** and **5_I** (the flanking tolyl units and the chlorine atom being displaced on the same side with respect to the central ring, see Figures S43 and S44) are the ones identified in solid-state. However, the low energy differences between these isomers further emphasize the rotameric behaviour of sulfone ligands, even when coordinated to Ge/Sn atoms in metallylenes. On the other hand, for both **4** and **5** the best correlations with the experimental data were found for calculations performed in THF.

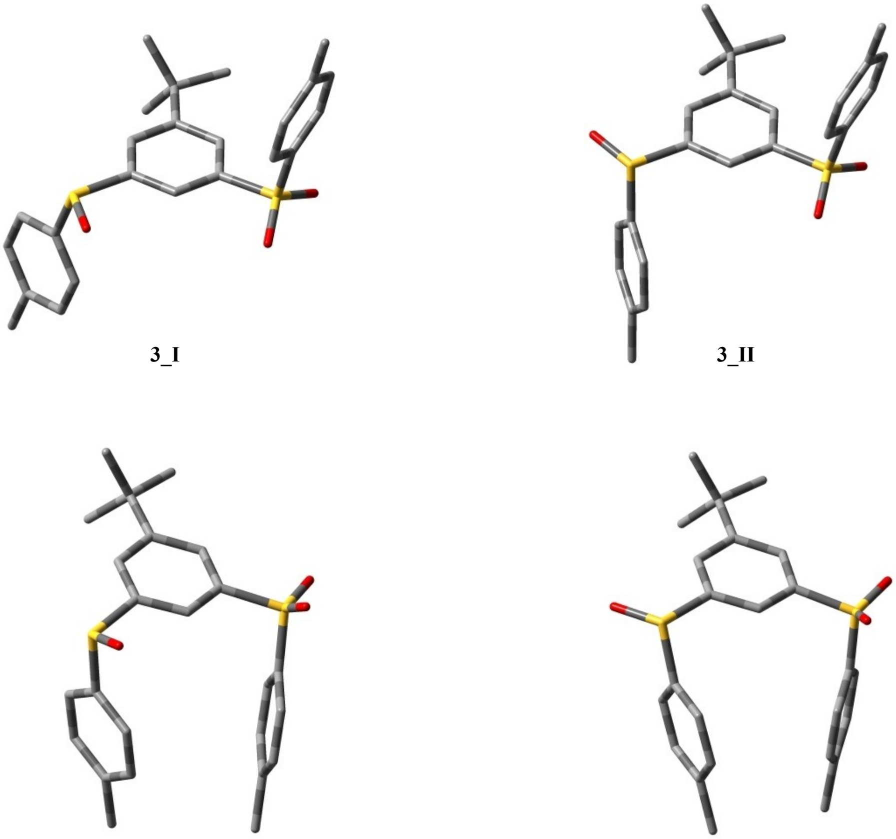

3_I 3_II

3_III 3_IV

Figure S42. Molecular geometries corresponding to the analysed isomers of the sulfone-sulfoxide ligand **3**, for *trans*- (**3_I** and **3_II**) and *cis*- (**3_III** and **3_IV**) orientation of the tolyl units. Hydrogen atoms were omitted for better clarity.

Table S5. DFT calculated energies of the investigated isomers of **3** in gaseous phase and solvent (toluene, THF and acetone).

	Gaseous Phase		**Toluene**		**THF**		**Acetone**	
Isomer	**Sum of electronic and thermal Energies (a.u.)**	**ΔE (kcal/mol)**	**Sum of electronic and thermal Energies (a.u.)**	**ΔE (kcal/mol)**	**Sum of electronic and thermal Energies (a.u.)**	**ΔE (kcal/mol)**	**Sum of electronic and thermal Energies (a.u.)**	**ΔE (kcal/mol)**
3_I	-1952.316787	**0.0**	-1952.325415	**0.0**	-1952.332307	**0.0**	-1952.33511	**0.0**
3_II	-1952.317865	**-0.7**	-1952.326085	**-0.4**	-1952.332539	**-0.1**	-1952.335083	**0.0**
3_III	-1952.316302	**0.3**	-1952.325253	**0.1**	-1952.332492	**-0.1**	-1952.336452	**-0.8**
3_IV	-1952.31953	**-1.7**	-1952.327976	**-1.6**	-1952.335012	**-1.7**	-1952.337686	**-1.6**

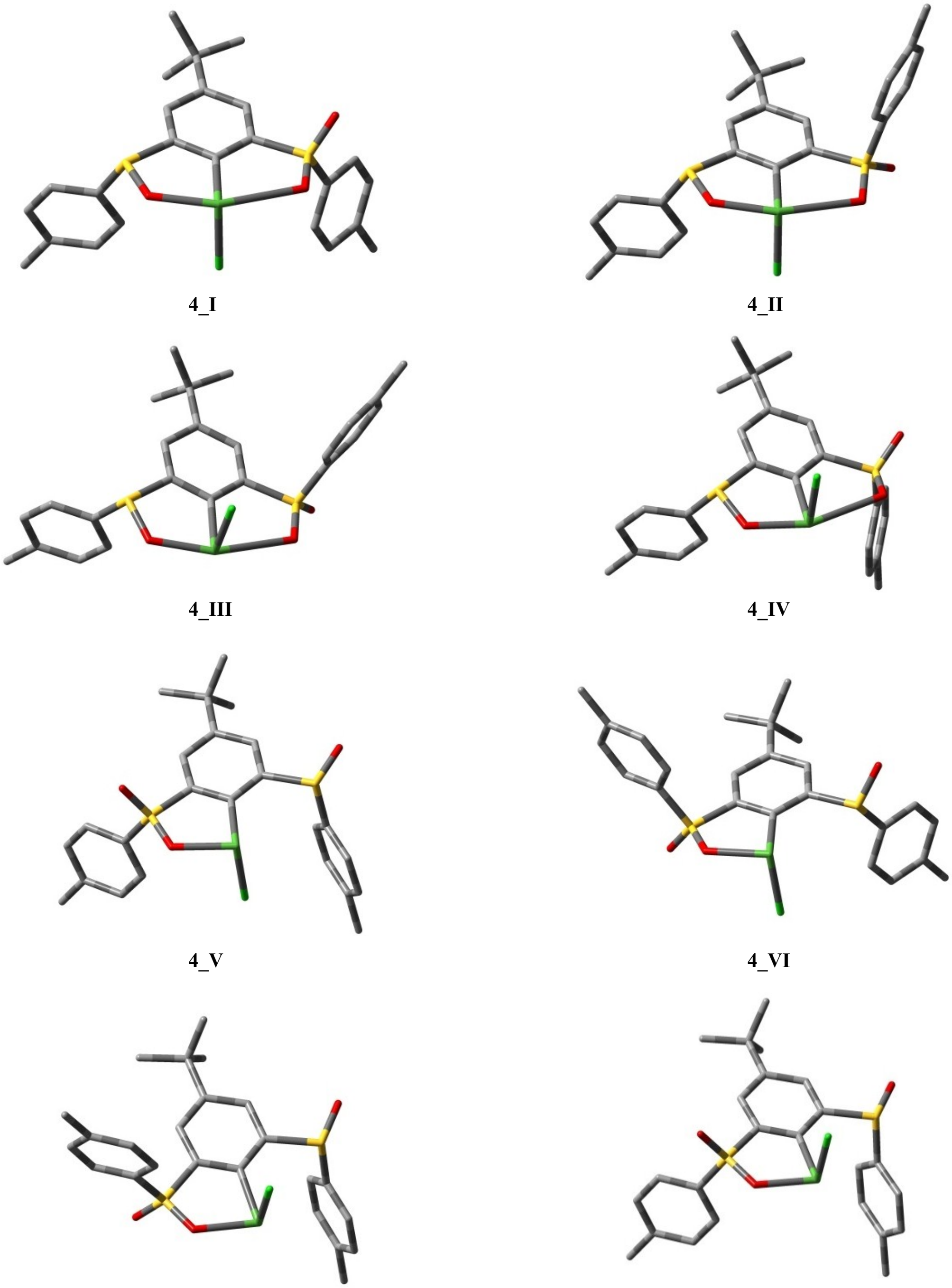

4_I

4_II

4_III

4_IV

4_V

4_VI

4_VII

4_VIII

Figure S43. DFT optimized molecular structures of to the investigated isomers of sulfone-sulfoxide germylene **4**; hydrogen atoms were omitted for enhanced clarity.

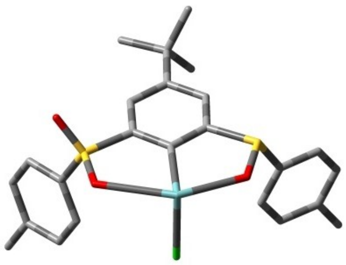

5_I

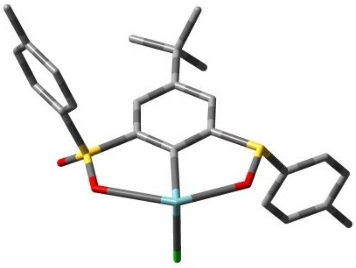

5_II

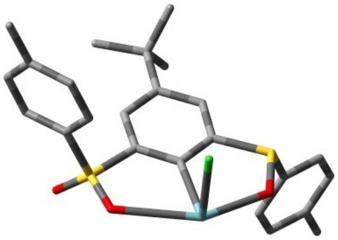

5_III

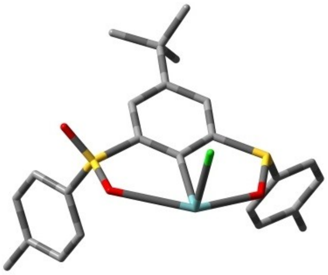

5_IV

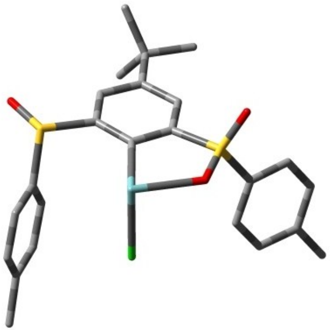

5_V

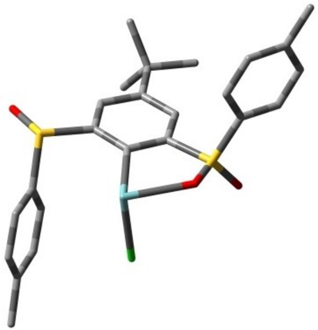

5_VI

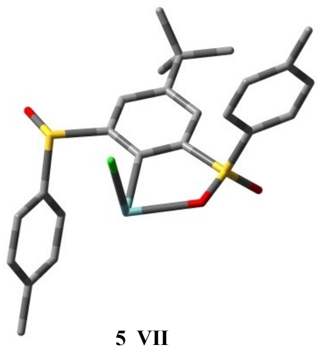

5_VII

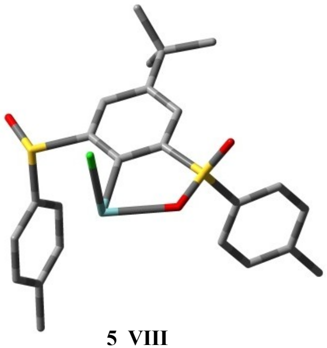

5_VIII

Figure S44. DFT optimized molecular structures of to the analysed isomers of sulfone-sulfoxide stannylene **5**; hydrogen atoms were omitted for clarity.

Table S6. Calculated energies of species **4_I** – **4_VIII** (the sulfone-sulfoxide germylene's isomers) as obtained at the B3LYP-D3/Def2-TZVP level of theory in gaseous phase, toluene and THF.

Isomer	Gaseous Phase		Toluene		THF	
	Sum of electronic and thermal Energies (a.u.)	ΔE (kcal/mol)	Sum of electronic and thermal Energies (a.u.)	ΔE (kcal/mol)	Sum of electronic and thermal Energies (a.u.)	ΔE (kcal/mol)
4_I	-4489.071164	**0.0**	-4489.080303	**0.0**	-4489.088178	**0.0**
4_II	-4489.067184	**2.5**	-4489.077303	**1.9**	-4489.086062	**1.3**
4_III	-4489.067812	**2.1**	-4489.078016	**1.4**	-4489.086467	**1.1**
4_IV	-4489.063578	**4.8**	-4489.074800	**3.5**	-4489.084541	**2.3**
4_V	-4489.058869	**7.7**	-4489.065686	**9.2**	-4489.072223	**10.0**
4_VI	-4489.055055	**10.1**	-4489.064200	**10.1**	-4489.071595	**10.4**
4_VII	-4489.056901	**9.0**	-4489.065639	**9.2**	-4489.072168	**10.0**
4_VIII	-4489.052308	**11.8**	-4489.061983	**11.6**	-4489.070119	**11.3**

Table S7. Calculated energies of species **5_I** – **5_VIII** (the sulfone-sulfoxide stannylene's isomers) as delivered by B3LYP-D3/Def2-TZVP calculations carried out in gaseous phase, toluene and THF.

Isomer	Gaseous Phase		Toluene		THF	
	Sum of electronic and thermal Energies (a.u.)	ΔE (kcal/mol)	Sum of electronic and thermal Energies (a.u.)	ΔE (kcal/mol)	Sum of electronic and thermal Energies (a.u.)	ΔE (kcal/mol)
5_I	-2626.424345	**0.0**	-2626.432787	**0.0**	-2626.439886	**0.0**
5_II	-2626.419109	**3.3**	-2626.428758	**2.5**	-2626.437142	**1.7**
5_III	-2626.420217	**2.6**	-2626.429903	**1.8**	-2626.437811	**1.3**
5_IV	-2626.414608	**6.1**	-2626.425639	**4.5**	-2626.435139	**3.0**
5_V	-2626.407913	**10.3**	-2626.416460	**10.2**	-2626.423302	**10.4**
5_VI	-2626.403199	**13.3**	-2626.41293	**12.5**	-2626.421127	**11.8**
5_VII	-2626.406362	**11.3**	-2626.415526	**10.8**	-2626.42269	**10.8**
5_VIII	-2626.400844	**14.7**	-2626.411017	**13.7**	-2626.419948	**12.5**

The best correlation between the solid-state determined *O(sulfoxide)→M* and *O(sulfone)→M* lengths (M=Ge,Sn) and the calculated ones was notices for calculations performed in THF, for both **4_I** and **5_I** isomers (Tables S8 and S9). Comparable distances were calculated for the coordinative bonds in the series of **4_I-4_IV** and **5_I-5_IV** isomers. For species **4_V-4_VIII** and **5_V-5_VIII,** *O(sulfone)→M* bonds are significantly shorter, in order to compensate the lack of *O(sulfoxide)→M* (Tables S8 and S9).

Table S8. Calculated lengths of *O(sulfoxide)→Ge* and *O(sulfone)→Ge* coordinative bonds within isomers **4_I** – **4_VIII**; DFT calculations were performed in gaseous phase, toluene and THF.

Isomer	Gaseous Phase		Toluene		THF	
	O(sulfoxide)→Ge (Å)	O(sulfone)→Ge (Å)	O(sulfoxide)→Ge (Å)	O(sulfone)→Ge (Å)	O(sulfoxide)→Ge (Å)	O(sulfone)→Ge (Å)
4_I	2.150	2.658	2.114	2.696	2.082	2.724
4_II	2.139	2.701	2.102	2.735	2.076	2.750
4_III	2.155	2.658	2.111	2.699	2.081	2.720
4_IV	2.125	2.796	2.087	2.803	2.065	2.795
4_V	–	2.142	–	2.117	–	2.113
4_VI	–	2.148	–	2.133	–	2.119
4_VII	–	2.128	–	2.135	–	2.107
4_VIII	–	2.134	–	2.120	–	2.119

Table S9. Calculated distances of *O(sulfoxide)→Sn* and *O(sulfone)→Sn* coordinative bonds within isomers **5_I** – **5_VIII**; DFT calculations were performed in gaseous phase, toluene and THF.

Isomer	Gaseous Phase		Toluene		THF	
	O(sulfoxide)→Sn (Å)	**O(sulfone)→Sn (Å)**	**O(sulfoxide)→Sn (Å)**	**O(sulfone)→Sn (Å)**	**O(sulfoxide)→Sn (Å)**	**O(sulfone)→Sn (Å)**
5_I	2.372	2.650	2.349	2.669	2.328	2.686
5_II	2.368	2.670	2.348	2.677	2.329	2.686
5_III	2.376	2.652	2.344	2.677	2.322	2.692
5_IV	2.355	2.734	2.329	2.730	2.314	2.720
5_V	–	2.311	–	2.311	–	2.308
5_VI	–	2.321	–	2.316	–	2.310
5_VII	–	2.326	–	2.322	–	2.316
5_VIII	–	2.316	–	2.310	–	2.305

NBO calculations were performed on the most stable isomers from each series: **4_I-4_IV** and **5_I-5_IV**. The calculated values of the donor-acceptor interactions associated with the *O(sulfoxide)→M* and *O(sulfone)→M* coordinative bonds (M=Ge,Sn) are presented in Tables S10 and S11. Data were obtained from the second order perturbation theory analysis of the NBO calculations, and represent a sumation of all charge transfer interactions of the type LP(O)→*p*(M) for each *O→M* bond (M=Ge,Sn).

Table S10. The calculated donor-acceptor energies of the *O(sulfoxide)→Ge* and *O(sulfone)→Ge* coordinative bonds in isomers **4_I**, **4_II**, **4_III** and **4_IV**; energetic values computed from the second order perturbation theory analyses of NBO calculations.

Isomer	Gaseous Phase		Toluene		THF	
	p_{O}**(sulfoxide)→**p_{Ge} **(kcal/mol)**	p_{O}**(sulfone)→**p_{Ge} **(kcal/mol)**	p_{O}**(sulfoxide)→**p_{Ge} **(kcal/mol)**	p_{O}**(sulfone)→**p_{Ge} **(kcal/mol)**	p_{O}**(sulfoxide)→**p_{Ge} **(kcal/mol)**	p_{O}**(sulfone)→**p_{Ge} **(kcal/mol)**
4_I	74.3	18.8	79.9	16.7	84.8	15.2
4_II	76.7	17.1	82.4	15.4	86.2	14.5
4_III	73.9	18.9	81.6	16.5	86.9	15.4
4_IV	77.6	13.1	85.1	12.7	89.9	13.0

Table S11. The calculated donor-acceptor energies of the *O(sulfoxide)→Sn* and *O(sulfone)→Sn* coordinative bonds in isomers **5_I**, **5_II**, **5_III** and **5_IV**; energetic values computed from the second order perturbation theory analyses of NBO calculations.

Isomer	Gaseous Phase		Toluene		THF	
	p_{O}**(sulfoxide)→**p_{Sn} **(kcal/mol)**	p_{O}**(sulfone)→**p_{Sn} **(kcal/mol)**	p_{O}**(sulfoxide)→**p_{Sn} **(kcal/mol)**	p_{O}**(sulfone)→**p_{Sn} **(kcal/mol)**	p_{O}**(sulfoxide)→**p_{Sn} **(kcal/mol)**	p_{O}**(sulfone)→**p_{Sn} **(kcal/mol)**
5_I	47.8	20.2	51.0	18.9	53.8	17.8
5_II	48.8	19.2	51.6	18.7	54.2	18.0
5_III	47.1	20.1	52.1	18.4	55.5	17.5
5_IV	48.5	15.6	53.0	15.7	56.2	16.1

Nucleus independent chemical shift (NICS) calculations were carried out on isomers **4_I** and **5_I**, in gaseous phase, toluene and THF. Calculations were performed on the chelate rings formed by oxygen coordination to M (M=Ge,Sn) and on the central phenyl ring. The NICS(0) and NICS(1) values were computed, in which the ghost atom is displeced in the midle of the ring (centroid) and 1 Å above the ring centroid, respectivly (Table S12). The benzene molecule was set as reference, NICS calculations being carried out on it at the same DFT level of theory as for **4_I** and **5_I**.

Table S12. NICS(0) and NICS(1) calculated values for the chelate rings formed by *O(sulfoxide)→M* and *O(sulfone)→M* coordinations (M=Ge,Sn) and of the central phenyl cycle of species **4_I** and **5_I**.

	Isomer	**Chelate ring with sulfoxide**		**Chelate ring with sulfone**		**Central phenyl ring**		**Benzene reference values**	
		NICS(0)	**NICS(1)**	**NICS(0)**	**NICS(1)**	**NICS(0)**	**NICS(1)**	**NICS(0)**	**NICS(1)**
Gas	**4_I**	-1.46	-1.45	0.58	-0.29	-9.46	-10.14	**-8.12**	**-10.01**
	5_I	-1.18	-1.28	0.37	-0.35	-9.33	-10.16		
Tol	**4_I**	-1.48	-1.49	0.65	-0.21	-9.40	-10.10	**-8.10**	**-10.00**
	5_I	-1.20	-1.28	0.37	-0.32	-9.31	-10.12		
THF	**4_I**	-1.47	-1.59	0.75	-0.13	-9.26	-10.00	**-8.02**	**-10.03**
	5_I	-1.22	-1.28	0.39	-0.26	-9.28	-10.07		

However, a more widely accepted criterion for measuring aromaticity is represented by the NICS$_{ZZ}$ value. As aromaticity is a property of the π-electrons, the ZZ magnetic component (perpendicular on the molecular plane - the XY plane) is regarded as a better measurement than the isotropic value. Hence, the calculated NICS$_{ZZ}$(2) values for the chelate and central rings in **4_I** and **5_I** are presented in Table S13 (data is presented for calculations carried out in gaseous phase, similar values were obtained for those performed in toluene and THF).

Table S13. NICS$_{ZZ}$(2) calculated values for the chelate rings formed by *O(sulfoxide)→M* and *O(sulfone)→M* (M=Ge,Sn) coordinations and of the central phenyl ring of species **4_I** and **5_I** in gaseous phase.

	Isomer	**Chelate ring with sulfoxide**	**Chelate ring with sulfone**	**Central phenyl ring**	**Benzene reference values**
		NICS$_{ZZ}$(2)	**NICS$_{ZZ}$(2)**	**NICS$_{ZZ}$(2)**	**NICS$_{ZZ}$(2)**
Gas	**4_I**	-6.21	-4.10	-15.63	**-17.48**
	5_I	-6.19	-4.41	-15.74	

The values illustrated in Tables S12 and S13 suggest (low) *quasi*-aromatic behaviour, especially for the chelate rings formed with the sulfoxide unit in both **4_I** and **5_I**. Nevertheless, the aromatic character is much lower than of the central phenyl ring or of the reference benzene molecule.

References:

[1] M. El Ezzi, R. Lenk, D. Madec, J.-M. Sotiropoulos, S. Mallet-Ladeira, A. Castel, *Angew. Chem. Int. Ed.*, **2015**, *54*, 805–808.